JOINT GRADIENT BALANCING FOR DATA ORDERING IN FINITE-SUM MULTI-OBJECTIVE OPTIMIZATION

Hansi Yang, James Kwok
Department of Computer Science and Engineering,
The Hong Kong University of Science and Technology, Hong Kong, China
{hyangbw, jamesk}@cse.ust.hk

ABSTRACT

In finite-sum optimization problems, the sample orders for parameter updates can significantly influence the convergence rate of optimization algorithms. While numerous sample ordering techniques have been proposed in the context of single-objective optimization, the problem of sample ordering in finite-sum multi-objective optimization has not been thoroughly explored. To address this gap, we propose a sample ordering method called JoGBa, which finds the sample orders for multiple objectives by jointly performing online vector balancing on the gradients of all objectives. Our theoretical analysis demonstrates that this approach outperforms the standard baseline of random ordering and accelerates the convergence rate for the MGDA algorithm. Empirical evaluation across various datasets with different multi-objective optimization algorithms further demonstrates that JoGBa can achieve faster convergence and superior final performance than other data ordering strategies.

1 INTRODUCTION

Many well-known machine learning problems involve jointly optimizing multiple objectives in model training. Examples include multi-task learning (Sener & Koltun, 2018), meta-learning (Ye et al., 2021), learning with fairness and safety constraints (Zafar et al., 2017) and multi-agent reinforcement learning (Moffaert & Nowé, 2014). Mathematically, these problems share the same formulation of minimizing a vector-valued loss function $\mathcal{L}$ and can be defined as:

$$\min_{\boldsymbol{w}\in\mathbb{R}^d} \ \mathcal{L}(\boldsymbol{w}) \coloneqq [\mathcal{L}_1(\boldsymbol{w}), \ldots, \mathcal{L}_M(\boldsymbol{w})]. \tag{1}$$

Here, each loss function $\mathcal{L}_m(\boldsymbol{w}), m = 1, \ldots, M$ corresponds to a training objective and can be expressed by $\mathcal{L}_m(\boldsymbol{w}) = \sum_{n=1}^{N} \ell_m(\boldsymbol{w}, \xi_n)$, where each ξ_n denotes a training sample and ℓ_m is the per-sample loss. Solving problem (1) is fundamentally different from common single-objective optimization problems as different objectives may have conflicts with each other. A straight-forward baseline is to optimize a weighted average of the multiple objectives, also known as *static or unitary weighting* (Kurin et al., 2022; Xin et al., 2022). Its performance then largely depends on how to choose the weights to balance different objectives, and may involve huge amount of tuning efforts. A popular alternative is thus to *dynamically weight* gradients from different objectives to avoid conflicts between them. Generally, these methods share the same procedure: First, compute all the gradients of each objective, then compute a set of weights for different objectives based on their gradients. The model is updated by the weighted sum of all gradients, while the weights can dynamically change. The pioneering work of this approach is the multi-gradient descent algorithm (MGDA) (Désidéri, 2012) and its stochastic variants (Liu & Vicente, 2021; Fernando et al., 2023; Zhou et al., 2022; Chen et al., 2024). Later works further improve upon MGDA by considering the worst improvement among different objectives (Liu et al., 2021; Ban & Ji, 2024), as well as constructing a bargaining game between different objectives (Navon et al., 2022).

While the aforementioned methods can be used to compute weights dynamically based on the loss gradients, a less-investigated issue for finite-sum multi-objective optimization is how we order the samples to compute their gradients and solve the problem in (1) with stochastic optimization. For

single-objective optimization in the finite-sum setting, many methods have been proposed for ordering the samples (Ying et al., 2017; Gürbüzbalaban et al., 2019; Lu et al., 2021; Mohtashami et al., 2022; Lu et al., 2022). With multiple objectives, a simple generalization of existing single-objective sample ordering methods is to treat the weighted average of all loss gradients as sample "gradient" for update (Figure 1(a)). However, the gradient weights may change drastically during model update, making existing methods unstable and often do not outperform the simple baseline of random ordering. Another simple extension is to run the single-objective sample ordering algorithm on each objective separately, but this can lead to different orderings for different objectives (Figure 1(b)). Moreover, it overlooks possible conflicts between gradients from different samples, and thus may still yield limited improvement over random ordering.

Motivated by the above limitations, in this paper, we propose a novel sample ordering framework for multi-objective optimization. As illustrated in Figure 1(c), the proposed method jointly provides sample orderings for different objectives by solving an online vector balancing problem with the gradients on each objective. The online vector balancing problem allows us to control the maximum norm of total model update in each epoch, leading to the theoretical guarantee of accelerated convergence. Specifically, our theoretical results demonstrate that the proposed method improves over the random ordering baseline for finite-sum multi-objective optimization, with smaller sample variance and faster convergence. Empirical results on a variety of data sets with multiple learning objectives demonstrate that the proposed method achieves faster convergence and better performance than the other data sampling methods.

Our contributions can be summarized as follows:

- We propose a novel data ordering method that uses gradient balancing across different objectives to accelerate convergence.
- We propose a novel theoretical framework to analyze multi-objective optimization with different data ordering for each objective.
- Empirical results on various multi-task learning data sets demonstrate effectiveness of the proposed method.

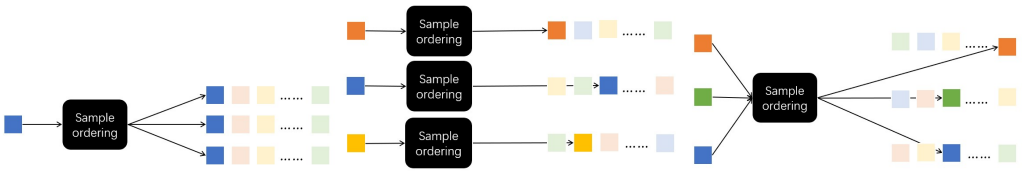

(a) Same ordering for all objectives. (b) Data ordering on each objective separately. (c) Proposed method: joint data ordering on all objectives.

Figure 1: Visualization of different data ordering approaches for multi-objective optimization.

2 Related Works

2.1 Permutation-based SGD for Finite-Sum Optimization

In an online setting, training samples are often assumed to be sampled independently from an underlying distribution. However, such asssumption does not match actual implementation that uses finite training samples in an order. Instead, permutation-based SGD proposes to first sort all the training samples by an order, and then use the samples following this order. An example is random reshuffling (Ying et al., 2017) and the related shuffle-once method (Bertsekas, 2011; Gürbüzbalaban et al., 2019), which first generates a random permutation of all the training samples in each epoch, and then uses the training samples following this order in the subsequent iterations. Theoretical analysis of random reshuffling dates back to Recht & Ré (2012). Rajput et al. (2021) introduce a variant of random reshuffling that reverses the order every two epochs, and theoretically demonstrates that this variant achieves faster convergence for quadratic objectives.

Instead of using a random order, Lu et al. (2021),Mohtashami et al. (2022), and Lu et al. (2022) try to find better sample orders. These works are mostly based on the herding problem (Welling, 2009), which minimizes the consecutive errors of stochastic gradients. Theoretical analysis (Cha et al.,

2023) demonstrates that the ordering based on the herding problem is asymptotically optimal. There are different methods to solve the herding problem. Mohtashami et al. (2022) evaluates gradients on all samples first and then solves the herding problem to obtain the order for all samples before starting an epoch. Lu et al. (2021) uses stale gradients from the previous epoch to estimate the gradient on each sample. Lu et al. (2022) proposes to solve the herding problem via online vector balancing, which removes the additional storage cost in (Mohtashami et al., 2022; Lu et al., 2021).

Despite the aforementioned improvements, existing works on permutation-based SGD only focus on single-objective optimization problems. While some simple extensions exist for training with multiple objectives (e.g., by using the weighted gradient or ordering samples for each objective separately), these simple extensions do not always yield much improvements, as will be demonstrated in our empirical results.

2.2 Gradient-based Multi-objective Optimization

To balance the optimization on different objectives, most existing algorithms use the weighted average of all objective gradients to update the model. There are different ways to compute the weights for different objectives. Some works perform the weighting based on some heuristics. Examples include using the prediction uncertainty (Kendall et al., 2017), gradient norms (Chen et al., 2018) or task difficulty (Guo et al., 2018). Another line of works propose to compute the objective weights from some sub-problems on the objective gradients. The pioneering work is MGDA (Désidéri, 2012), which computes the weights by avoiding conflicts across any objective. Stochastic variants of MGDA with optimization convergence guarantees have been proposed in (Liu & Vicente, 2021; Zhou et al., 2022; Fernando et al., 2023; Chen et al., 2024). PCGrad (Yu et al., 2020) proposes to project the gradients of tasks to the normal plane of the other tasks with conflicting gradients. CA-Grad (Liu et al., 2021) searches for an update direction in a neighborhood of the average gradient that maximizes the worst improvement of any task. Nash-MTL (Navon et al., 2022) proposes to look for a fair gradient direction based on a bargaining game between different objectives.

Convergence analysis for the deterministic MGDA algorithm dates back to (Fliege et al., 2019). Later on, stochastic variants of MGDA are introduced (Liu & Vicente, 2021; Zhou et al., 2022; Fernando et al., 2023; Chen et al., 2024). However, the vanilla stochastic MGDA introduces a biased estimate of the dynamic weight, which results in the biased estimate of update direction during optimization. To address this issue, Liu & Vicente (2021) propose to increase the batch size during optimization, and prove the convergence of stochastic MGDA with the Lipschitz continuity assumption on the objective weights $\lambda^*(\boldsymbol{w})$ with respect to the loss gradients $\nabla\mathcal{L}(\boldsymbol{w})$. Nevertheless, as first proved in (Zhou et al., 2022, Proposition 2), this assumption does not hold in general. To address this problem, momentum-based bias reduction algorithms (Zhou et al., 2022; Fernando et al., 2023) are proposed to eliminate such unrealistic assumptions. The convergence of the MGDA algorithm without the unrealistic Lipschitzness assumption is first established in (Chen et al., 2024), which propose to mitigate the bias in update direction via double sampling. Most existing works focus on the convergence analysis under an online setting instead of the finite-sum setting, and ignores the impact of sample orders in their theoretical analysis.

3 Proposed Method

3.1 Multiple Sample Orderings for Multiple Objectives

A simple extension of existing single-objective sample ordering methods to multi-objective optimization is to use the weighted average of all loss gradients as the sample "gradient", and follow existing data ordering methods on the weighted gradient. When the objective weights do not change with different samples, this extension can be regarded as using the weighted objective as the only objective in the existing methods. However, since the objective weights are constantly changing, using the same sample order cannot well tackle the possible conflicts between different objectives.

To alleviate this problem, we propose to use different sample orders for different objectives. Specifically, for a data set with K samples, we generate an order $\pi_t^m : \{1, \dots, K\} \to \{1, \dots, K\}$ for the m-th objective. Some simple methods to generate the order π_t^m in each epoch t are listed below:

1. Random: In each epoch t, the data sets are randomly shuffled to generate an ordering π_t^m for each objective.
2. FlipFlop: For each objective, create a new order π_{t+1}^m by reversing the previous π_t^m, i.e., $\pi_{t+1}^m(k) = \pi_t^m(K+1-k)$.
3. Random FlipFlop, which performs Random on even epochs and FlipFlop on odd epochs.

3.2 Sample Ordering by Online Vector Balancing

Despite the simple ordering methods introduced in Section 3.1, some recent works (Lu et al., 2021; Mohtashami et al., 2022; Lu et al., 2022) propose to adaptively find a good order for all training samples in each epoch for faster convergence with a single objective. An example is GraB (Lu et al., 2022), which tries to find a sample ordering π that minimizes the maximum norm of parameter update in each epoch, i.e., $\max_{K'} \|\boldsymbol{w}^{(K')} - \boldsymbol{w}^{(1)}\|_\infty$. With a single objective ℓ, the model parameters are updated by $\boldsymbol{w}^{(k+1)} = \boldsymbol{w}^{(k)} - \alpha \nabla \ell(\boldsymbol{w}, \xi_{\pi(k)})$ at each iteration k in an epoch. This problem is then transformed to the online vector balancing problem defined below:

Definition 3.1 (Online Vector Balancing (Spencer, 1977))**.** Given K vectors $\{\boldsymbol{z}_k\}_{k=1}^K \in \mathbb{R}^d$, arriving one at a time, the goal of *online vector balancing* is to assign a sign $\epsilon_k \in \{-1, +1\}$ to each vector upon receiving it so as to minimize $\max_{m \in \{1,\dots,K\}} \| \sum_{k=1}^m \epsilon_k \boldsymbol{z}_k \|_\infty$.

We propose to generalize this problem to multiple objectives by replacing the gradients on a single objective to those on multiple obejctives and jointly consider their influence to the model updates. The complete procedure, called JoGBa (**Jo**int **G**radient **Ba**lancing), is shown in Algorithm 1. Specifically, at the k-th iteration of epoch t, we compute the gradients $\{\nabla \ell_m(\boldsymbol{w}_t^{(k)}, \xi_{\pi_t^m(k)})\}_{m=1}^M$ for all M objectives w.r.t. the current model parameter $\boldsymbol{w}_t^{(k)}$. The sample order π^m for each objective is then determined by solving the balancing problem on the gradients from different objectives, implemented by routine `Balancing` in step 11. While there exists different ways to solve the online vector balancing problem and compute the gradient sign $\epsilon_{m,k,t}$, here we follow GraB and use a greedy algorithm that works well in practice. As shown in Algorithm 2, we compare two vector norms $\|\boldsymbol{s} + \boldsymbol{g}_{m,k,t}\|_\infty$ and $\|\boldsymbol{s} - \boldsymbol{g}_{m,k,t}\|_\infty$, where $\boldsymbol{s} + \boldsymbol{g}_{m,k,t}$ corresponds to putting this sample at the beginning and $\boldsymbol{s} - \boldsymbol{g}_{m,k,t}$ corresponds to putting this sample at the end. Since the online vector balancing problem in Definition 3.1 tries to minimize the vector sum's norm, we choose the sample order that can lead to the smallest norm, as is indicated by the value of $\epsilon_{m,k,t}$. The vector $\boldsymbol{s}$ is shared among different objectives to enable joint balancing across their corresponding gradients. After the balancing routine is complete, we compute the objective weights λ by any multi-task learning algorithm (routine MTL), such as MGDA (Désidéri, 2012) or Nash-MTL (Navon et al., 2022). We then update the mean $\boldsymbol{v}$ of all gradients and perform model update on $\boldsymbol{w}_t^{(k)}$.

3.3 Theoretical Analysis

In this section, we theoretically demonstrate how Algorithm 1 improves upon simple extensions of sample ordering methods to multi-objective optimization. Since the convergence analysis of multi-objective optimization is different from optimizing a single objective, we first introduce the definition of Pareto stationary. Denote the gradients for all M objectives as $\nabla \mathcal{L}(\boldsymbol{w}) \in \mathbb{R}^{d \times M}$, where $\mathcal{L}(\boldsymbol{w})$ is defined as in (1), and define Δ^M as the following set:

$$\Delta^M \coloneqq \left\{ \lambda \in \mathbb{R}^M : \sum\nolimits_{m=1}^M \lambda_m = 1, \lambda_m \geq 0, \forall m = 1, \dots, M \right\}.$$

Analogous to the stationary and optimal solutions for a single objective, we define Pareto stationary and Pareto-optimal solutions for the multi-objective optimization problem $\min_{\boldsymbol{w} \in \mathbb{R}^d} \mathcal{L}(\boldsymbol{w})$.

Definition 3.2 (Pareto stationary and Pareto optimality (Momma et al., 2022))**.** If there exists a convex combination of the gradient vectors that equals to zero, i.e., there exists $\lambda \in \Delta^M$ such that $\nabla \mathcal{L}(\boldsymbol{w})\lambda = 0$, then $\boldsymbol{w} \in \mathbb{R}^d$ is *Pareto stationary* for $\mathcal{L}$. If there is no $\boldsymbol{w} \in \mathbb{R}^d$ and $\boldsymbol{w} \neq \boldsymbol{w}^*$ such that, for all $\mathcal{L}_m(\boldsymbol{w})$ defined in (1) with $m = 1, \dots, M$, $\mathcal{L}_m(\boldsymbol{w}) \leq \mathcal{L}_m(\boldsymbol{w}^*)$, and for at least a $m' = 1, \dots, M$, $\mathcal{L}_{m'}(\boldsymbol{w}) < \mathcal{L}_{m'}(\boldsymbol{w}^*)$, then $\boldsymbol{w}^*$ is *Pareto optimal* for $\mathcal{L}$.

By definition, at a Pareto stationary point, there is no common descent direction for all objectives. A necessary and sufficient condition for $\boldsymbol{w}$ being Pareto stationary for smooth objectives is that

Algorithm 1 JoGBa: **Jo**int **G**radient **Ba**lancing for Multi-Objective Optimization.

Input: number of epochs T, initialized order π_1, initialized weight $\boldsymbol{w}_0$, stale mean $\boldsymbol{v}_0 = \mathbf{0}$, step size α.
for $t = 0, \dots, T-1$ **do** $\{t$ is the number of epochs$\}$
  for $m = 1, \dots, M$ **do** $\{m$ is the index on different objectives$\}$
    Initialize left index $l_m \leftarrow 1$, right index $r_m \leftarrow K$
  end for
  Initialize running average $\boldsymbol{s} \leftarrow \mathbf{0}$, stale mean $\boldsymbol{v}_{t+1} \leftarrow \mathbf{0}$.
  for $k = 1, \dots, K$ **do** $\{k$ is the number of iterations in each epoch, $\pi_t^1(k), \dots, \pi_t^M(k)$ indicates the sample index we select for each objective$\}$
    Sample data $\xi_{\pi_t^1(k)}, \dots, \xi_{\pi_t^M(k)}$ from data set $\mathcal{D}$
    for $m = 1, \dots, M$ **do** {Compute the gradient on the m-th objective and updates its sample order π_{t+1}^m for next epoch $t+1$}
      Compute gradient $\nabla \ell_m(\boldsymbol{w}_t^{(k)}; \xi_{\pi_t^m(k)})$ and centered gradient $\boldsymbol{g}_{m,k,t} \leftarrow \nabla \ell_m(\boldsymbol{w}_t^{(k)}; \xi_{\pi_t^m(k)}) - \boldsymbol{v}_t$
      Compute sign for the current gradient: $\epsilon_{m,k,t} \leftarrow \texttt{Balancing}(\boldsymbol{s}, \boldsymbol{g}_{m,k,t})$
      if $\epsilon_{m,k,t} = +1$ **then**
        Update $\boldsymbol{s}$ and left index l_m: $\boldsymbol{s} \leftarrow \boldsymbol{s} + \boldsymbol{g}_{m,k,t}$; $\pi_{t+1}^m(l_m) \leftarrow \pi_t^m(k)$; $l_m \leftarrow l_m + 1$.
      else
        Update $\boldsymbol{s}$ and right index r_m: $\boldsymbol{s} \leftarrow \boldsymbol{s} - \boldsymbol{g}_{m,k,t}$; $\pi_{t+1}^m(r_m) \leftarrow \pi_t^m(k)$; $r_m \leftarrow r_m - 1$.
      end if
    end for
    Compute weights λ from multi-task learning algorithms $\lambda = \text{MTL}(\{\nabla \ell_m(\boldsymbol{w}_t^{(k)}; \xi_{\pi_t^m(k)})\}_{m=1}^M)$
    Update stale mean $\boldsymbol{v}_{t+1} \leftarrow \boldsymbol{v}_{t+1} + \frac{1}{K} \sum_{m=1}^M \nabla \ell_m(\boldsymbol{w}_t^{(k)}; \xi_{\pi_t^m(k)})$
    Optimizer Step: $\boldsymbol{w}_t^{(k+1)} \leftarrow \boldsymbol{w}_t^{(k)} - \alpha \sum_{m=1}^M \lambda_m \nabla \ell_m(\boldsymbol{w}_t^{(k)}; \xi_{\pi_t^m(k)})$
  end for
  Use the model parameter from last iteration as the initialization for next epoch $t+1$:$\boldsymbol{w}_{t+1}^{(1)} \leftarrow \boldsymbol{w}_t^{(K+1)}$.
end for

Algorithm 2 Online greedy implementation of $\texttt{Balancing}(\boldsymbol{s}, \boldsymbol{g}_{m,k,t})$.

Input: $\boldsymbol{s}, \boldsymbol{g}_{m,k,t}$.
$\epsilon_{m,k,t} = 1$ if $\|\boldsymbol{s} + \boldsymbol{g}_{m,k,t}\|_\infty \leq \|\boldsymbol{s} - \boldsymbol{g}_{m,k,t}\|_\infty$ else $\epsilon_{m,k,t} = -1$.
Return $\epsilon_{m,k,t}$.

$\min_{\lambda \in \Delta^M} \|\nabla \mathcal{L}(\boldsymbol{w})\lambda\| = 0$ (Tanabe et al., 2019), which corresponds to the stationary condition $\|\nabla \mathcal{L}_m(\boldsymbol{w})\| = 0$ for a specific objective $\mathcal{L}_m$. Then, similar to the gradient norm $\|\nabla \mathcal{L}_m(\boldsymbol{w})\|$ for single-objective optimization, the quantity $\min_{\lambda \in \Delta^M} \|\nabla \mathcal{L}(\boldsymbol{w})\lambda\|$ can be used as a measure of Pareto stationarity (Désidéri, 2012; Fliege et al., 2019; Liu & Vicente, 2021; Fernando et al., 2023).

Now we list several assumptions that are necessary for our theoretical results. These assumptions are all commonly used in previous theoretical analysis (Liu & Vicente, 2021; Fernando et al., 2023; Zhou et al., 2022; Chen et al., 2024) on the convergence of multi-objective optimization methods:

Assumption 3.3 (Lipschitzness of $\ell_m(\boldsymbol{w})$'s and $\mathcal{L}(\boldsymbol{w})$)**.** For all $m \in \{1, \dots M\}$, $\ell_m(\boldsymbol{w}, \xi)$ is f-Lipschitz continuous for all training samples ξ. $\mathcal{L}(\boldsymbol{w})$ is then F-Lipschitz continuous in the Frobenius norm with $F = \sqrt{M} f$.

Assumption 3.4 (Lipschitz smoothness of $\ell_m(\boldsymbol{w})$'s and $\mathcal{L}(\boldsymbol{w})$)**.** The gradient $\nabla \ell(\boldsymbol{w}, \xi)$ is f_1-Lipschitz continuous for all $m \in \{1, \dots, M\}$ for all ξ. $\nabla \mathcal{L}_m(\boldsymbol{w})$ is then F_1-Lipschitz continuous in the Frobenius norm with $F_1 = \sqrt{M} f_1$.

Assumption 3.5 (Bounded gradient variance for each objective)**.** For any $\boldsymbol{w}$ and sample ξ, the m-th loss function satisfies $\|\nabla \ell_m(\boldsymbol{w}, \xi) - \nabla \mathcal{L}_m(\boldsymbol{w})\|_2^2 \leq \sigma_m^2$ for some given σ_m.

We then have the following convergence result if we use the MGDA algorithm (Désidéri, 2012; Sener & Koltun, 2018) to compute the objective weights λ. Proof is in Appendix A.1.

Theorem 3.6 (Random Ordering)**.** *Suppose Assumptions 3.3, 3.4 and 3.5 hold. Define* $\Delta = \max_{\lambda \in \Delta^M} \mathcal{L}(\boldsymbol{w}_0)\lambda - \min_{\boldsymbol{w} \in \mathbb{R}^d, \lambda \in \Delta^M} \mathcal{L}(\boldsymbol{w})\lambda$ *as the maximum difference between objective values at initialization and that at Pareto optimality. Consider the model parameters*[1] $\{\boldsymbol{w}_t^{(1)}\}$ *gen-*

[1] Superscript 1 indicates the model parameters at the beginning of each epoch.

erated by the MGDA algorithm with random sample ordering. Set $\alpha = \sqrt{\frac{2\Delta}{F_1(F^2+\sigma^2)KT}}$ *where* $\sigma^2 = \max_m \sigma_m^2$ *with* σ_m^2 *defined in Assumption 3.5, then,*

$$\frac{1}{T}\sum_{t=0}^{T-1}\mathbb{E}\left[\min_{\lambda\in\Delta^M}\|\nabla\mathcal{L}(\boldsymbol{w}_t^{(1)})\lambda\|^2\right] \leq \sqrt{\frac{2F_1\Delta(F^2+\sigma^2)}{KT}} + \frac{\sigma^2(1+\log(T))}{T}. \tag{2}$$

To analyze the convergence rate of Algorithm 1 that uses online gradient balancing to determine sample ordering for different objectives, we first need an additional assumption on the `Balancing` subroutine, which is also used for gradient balancing with single objective in (Lu et al., 2022).

Assumption 3.7. (Balancing Bound) For the subroutine `Balancing` in Algorithm 1, denote its input vectors as $\boldsymbol{z}_1, \ldots, \boldsymbol{z}_n \in \mathbb{R}^d$ which satisfy $\|\boldsymbol{z}_i\|_2 \leq 1, \forall i = 1, \ldots n$. Suppose the subroutine assigns each vector $\boldsymbol{z}_i$ a sign $\epsilon_i \in \{-1, +1\}$. There exists a constant $A > 0$ such that $\|\sum_{i=1}^k \epsilon_i \boldsymbol{z}_i\|_\infty \leq A$ for all $k \in \{1, \ldots, n\}$.

From Definition 3.1, solving the online vector balancing problem corresponds to minimizing A in Assumption 3.7. We also have the following Proposition that controls the maximum norm of parameter updates in each epoch. Proof is in Appendix A.2.

Proposition 3.8. *Under Assumption 3.3 and 3.7 Algorithm 1 satisfies:* $\|\boldsymbol{w}_t^{(k)} - \boldsymbol{w}_t^{(1)}\|_\infty \leq AF$ *for all* $k \in \{1, \ldots, K\}$ *and* $t \in \{0, \ldots, T-1\}$.

Based on this Proposition, we can then prove the following convergence result.

Theorem 3.9. *Set*

$$\alpha = \min\left\{\sqrt[3]{\frac{\Delta}{32KA^2\sigma^2F_1^2T}}, \frac{1}{26(K+A)(F+F_1)}\right\}.$$

where $\sigma^2 = \max_m \sigma_m^2$ *with* σ_m^2 *defined in Assumption 3.5. Under Assumptions 3.3, 3.4 and 3.5, Algorithm 1 yields*

$$\frac{1}{T}\sum_{t=0}^{T-1}\mathbb{E}\left[\min_{\lambda\in\Delta^M}\|\nabla\mathcal{L}(\boldsymbol{w}_t^{(1)})\lambda\|^2\right] \leq 11\sqrt[3]{\frac{A^2F_1^2\Delta^2(F^2+\sigma^2)}{K^2T^2}} + \frac{\sigma^2}{T} + \frac{65\Delta(F+F_1)}{T} + \frac{8\Delta AF_1}{KT}.$$

Proof is in Appendix A.3. Compared to random ordering in Theorem 3.6, the convergence rate of Algorithm 1 has a different term $\mathcal{O}((KT)^{-2/3})$ on the right hand side, which is better than the $\mathcal{O}((KT)^{-1/2})$ term in Theorem 3.6. As such, Algorithm 1 can achieve faster convergence than random ordering as is implemented in existing multi-objective optimization methods. We also note that a smaller A leads to faster convergence, which demonstrates that solving the online vector balancing problem (minimizing A) is indeed useful to find better orders on the training samples.

The naive extension of GraB (Lu et al., 2022) that performs online vector balancing for gradients of each objective separately can also be analyzed under the same framework as follows:

Proposition 3.10 (Separate Ordering)**.** *Under Assumption 3.3 and 3.7, suppose that the sample order* π_t^m *in Algorithm 1 is separately generated for each objective. We have* $\|\boldsymbol{w}_t^{(k)} - \boldsymbol{w}_t^{(1)}\|_\infty \leq MAF$ *for all* $k \in \{1, \ldots, K\}$ *and* $t \in \{0, \ldots, T-1\}$.

Proof is in Appendix A.4. Compared to the results in Proposition 3.8, the bound here is M times larger if we apply gradient balancing separately on each objective. Recall that M is the total number of objectives. Thus, the convergence can be much slower than that in Theorem 3.9.

4 Experiments

In this section, we demonstrate the effectiveness of the proposed method for multi-objective optimization. We consider the following baselines: (i) Random reshuffling (Random), which is used in most existing implementations to randomly shuffle the whole data set in each epoch t, (ii) FlipFlop, which creates a new order π_{t+1} by reversing the previous order, i.e., $\pi_{t+1}(k) = \pi_t(K+1-k)$. (iii)

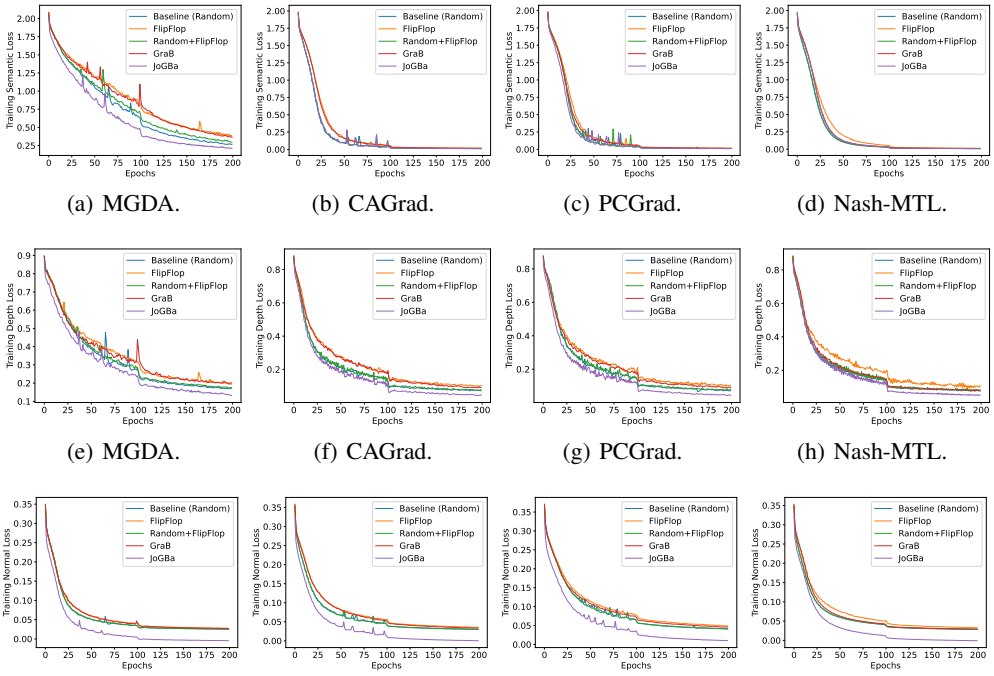

(a) MGDA. (b) CAGrad. (c) PCGrad. (d) Nash-MTL.

(e) MGDA. (f) CAGrad. (g) PCGrad. (h) Nash-MTL.

(i) MGDA. (j) CAGrad. (k) PCGrad. (l) Nash-MTL.

Figure 2: Training losses (objective values) of different tasks on NYUv2 data with different data ordering methods. Top: Loss on semantic segmentation task (semantic loss). Middle: Loss on depth estimation task (depth loss). Bottom: Loss on surface normal prediction task (normal loss).

Random FlipFlop, the combination of random reshuffling and FlipFlop, and (iv) GraB (Lu et al., 2022), which performs gradient balancing on the weighted gradient of all objectives, and the weight is computed using the combined dynamic weighting algorithm.

The proposed method is independent of the dynamic weighting algorithms. In the following, we combine it with a variety of dynamic weighting algorithms: (i) MGDA (Désidéri, 2012; Liu & Vicente, 2021; Zhou et al., 2022; Fernando et al., 2023), (ii) PCGrad (Yu et al., 2020), (iii) CAGrad (Liu et al., 2021), and (iv) Nash-MTL (Navon et al., 2022). We select these methods as they generally have good empirical performance. We also include a baseline STL (Single-Task Learning (Liu et al., 2021; Navon et al., 2022)) that directly trains on a task only and works as the upper bound for different multi-task learning methods. The proposed method can also be easily combined with other dynamic weighting algorithms.

We consider two data sets that are commonly used for multi-objective optimization in machine learning: (i) NYUv2 (Silberman et al., 2012), an indoor scene data set that involves three different tasks: semantic segmentation, depth estimation, and surface normal prediction. (ii) QM9 (Ramakrishnan et al., 2014), which is a widely used benchmark for graph neural networks predicting 11 properties of molecules. More details on the setup can be found in Appendix B.

4.1 NYUv2

Figure 2 compares the convergence curves of different ordering methods with the proposed method. We can see that the impact of sample orders on the convergence is generally different for different objectives. Both depth estimation and surface normal prediction tasks are more influenced by different sample ordering methods, while such influence becomes less significant for the semantic segmentation task. FlipFlop and GraB generally achieve worse performance than the other methods, while the proposed method JoGBa is the only one that can consistently outperform existing baselines with random ordering.

Table 1 compares the testing performance of different data ordering combined with different multi-objective optimization methods. FlipFlop generally performs worse than the other methods as it only reverses the sample ordering after each epoch. Random FlipFlop slightly improves upon the

Table 1: Test performance (averaged over 3 random seeds) for the three tasks on NYUv2 data: semantic segmentation, depth estimation, and surface normal prediction.

	Segmentation		Depth		Surface Normal					$\Delta\mathbf{m}\% \downarrow$
	mIoU ↑	Pix Acc ↑	Abs Err ↓	Rel Err ↓	Angle Distance ↓		Within t° ↑			
					Mean	Median	11.25	22.5	30	
STL	38.30	63.76	0.6754	0.2780	25.01	19.21	30.14	57.20	69.15	
MGDA (Random)	30.48	59.77	0.6020	0.2555	24.13	19.22	29.51	57.11	69.58	1.31
MGDA+FlipFlop	29.47	57.90	0.6270	0.2755	24.88	19.45	29.18	55.88	68.36	1.58
MGDA+Random FlipFlop	30.52	59.81	0.6018	0.2556	24.11	19.16	29.52	57.23	69.56	1.28
MGDA+GraB	30.74	59.92	0.6011	0.2524	24.12	19.11	29.54	57.35	69.76	1.25
MGDA+JoGBa	31.02	60.21	0.6008	0.2508	24.08	19.08	29.55	57.47	70.03	**1.19**
PCGrad (Random)	38.06	64.64	0.5550	0.2325	27.41	22.80	23.86	49.83	63.14	3.97
PCGrad+FlipFlop	37.74	64.63	0.5590	0.2285	26.84	22.19	23.96	49.30	62.94	3.89
PCGrad+Random FlipFlop	38.12	64.64	0.5570	0.2329	26.99	22.67	23.56	49.65	63.18	3.86
PCGrad+GraB	38.31	64.66	0.5552	0.2317	26.79	22.87	23.68	49.76	63.22	3.78
PCGrad+JoGBa	38.59	64.67	0.5545	0.2270	26.53	22.40	23.87	49.95	63.87	**3.56**
CAGrad (Random)	39.79	65.49	0.5486	0.2250	26.31	21.58	25.61	52.36	65.58	0.20
CAGrad+FlipFlop	39.42	65.55	0.5437	0.2219	25.79	21.75	25.97	52.17	65.34	0.27
CAGrad+Random FlipFlop	39.85	65.73	0.5467	0.2226	26.14	21.46	25.62	52.24	65.62	0.17
CAGrad+GraB	39.91	66.09	0.5428	0.2214	25.79	21.44	25.64	52.26	65.44	0.18
CAGrad+JoGBa	40.42	66.08	0.5410	0.2205	25.52	21.50	26.04	52.43	65.73	**0.03**
Nash-MTL (Random)	40.13	65.93	0.5261	0.2171	25.26	20.08	28.40	55.47	68.15	−4.04
Nash-MTL+FlipFlop	39.46	65.82	0.5313	0.2190	26.12	20.99	28.05	54.64	67.77	-3.88
Nash-MTL+Random FlipFlop	40.67	66.32	0.5184	0.2009	25.34	19.73	28.54	55.35	68.07	-4.16
Nash-MTL+GraB	40.84	66.51	0.5156	0.2087	25.26	19.45	28.62	55.37	68.11	-4.19
Nash-MTL+JoGBa	41.13	66.71	0.5112	0.2009	25.11	19.19	28.77	55.28	68.18	**-4.27**

standard random baseline. While GraB does not yield faster convergence rate in Figure 2, its testing performance is comparable to Random FlipFlop. The proposed method JoGBa achieves the best overall performance across different performance metrics for all three tasks.

4.2 QM9

Due to the large number of objectives in the QM9 data, here we only plot the average of all training objectives. The convergence curves are shown in Figure 3 for different sample ordering methods. Compared to the NYUv2 data set, the effect of sample ordering becomes less significant for the QM9 data. Only GraB and JoGBa achieve slight improvements than the other ordering methods.

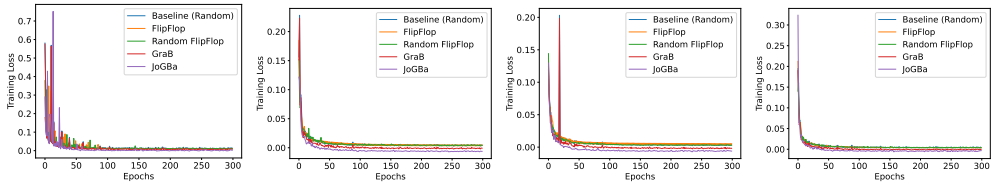

(a) MGDA. (b) CAGrad. (c) PCGrad. (d) Nash-MTL.

Figure 3: Training losses on QM9 data with different data ordering methods.

Table 2 compares the testing performance of different data ordering methods. Similar to the results for NYUv2, FlipFlop generally performs worse as it only reverses the sample ordering after each epoch. Random FlipFlop achieves comparable performance with the random ordering baseline, and GraB slightly improves upon it. The proposed method JoGBa achieves the best overall performance.

4.3 Comparison on Time Costs

The proposed JoGBa has two key steps in each iteration: (i) sample ordering, in which we determine the order of a sample based on its gradients, and (ii) model updating, in which we compute the objective weights and update the model with the weighted gradients. Table 3 compares the time costs of these two steps in each iteration for different multi-objective optimization algorithms on NYUv2 and QM9 data. As can be seen, the time cost of sample ordering is almost negligible compared to that of model update, and is generally the same for the same data set across different multi-objective optimization algorithms. This is intuitive as sample ordering is not related to any specific multi-objective optimization algorithm, and demonstrates that the proposed method does not introduce much additional time cost.

Table 2: Test performance (averaged over 3 random seeds) on all property prediction tasks in QM9.

	μ	α	ϵ_{HOMO}	ϵ_{LUMO}	$\langle R^2 \rangle$	ZPVE	U_0	U	H	G	c_v	
	MAE ↓											$\mathbf{\Delta_m}\% \downarrow$
STL	0.067	0.181	60.57	53.91	0.502	4.53	58.8	64.2	63.8	66.2	0.072	
MGDA (Random)	0.217	0.368	126.8	104.6	3.22	5.69	88.37	89.40	89.32	88.01	0.120	120.5
MGDA+FlipFlop	0.221	0.371	130.9	104.5	3.32	5.62	88.31	89.45	89.71	88.84	0.124	121.4
MGDA+Random FlipFlop	0.216	0.365	126.7	103.2	3.19	5.65	88.34	89.27	88.74	87.34	0.115	118.9
MGDA+GraB	0.206	0.343	120.8	101.4	3.16	5.44	87.68	88.63	88.87	87.26	0.119	118.4
MGDA+JoGBa	0.202	0.332	117.3	99.2	3.12	5.37	87.48	88.37	88.80	87.04	0.116	**116.7**
PCGrad (Random)	0.106	0.293	75.85	88.33	3.94	9.15	116.36	116.8	117.2	114.5	0.110	125.7
PCGrad+FlipFlop	0.106	0.306	75.15	88.29	3.87	9.17	120.17	117.4	117.8	114.1	0.113	126.3
PCGrad+Random FlipFlop	0.104	0.293	75.05	88.25	3.83	9.07	114.89	116.4	116.9	114.1	0.106	125.2
PCGrad+GraB	0.098	0.281	74.91	86.98	3.75	8.91	115.66	114.4	117.1	113.6	0.102	124.2
PCGrad+JoGBa	0.098	0.271	74.43	84.30	3.56	8.78	113.15	113.2	117.1	113.5	0.096	**123.5**
CAGrad (Random)	0.118	0.321	83.51	94.81	3.21	6.93	113.99	114.3	114.5	112.3	0.116	112.8
CAGrad+FlipFlop	0.115	0.325	85.13	94.94	3.24	7.09	114.32	115.2	114.9	113.1	0.117	113.1
CAGrad+Random FlipFlop	0.113	0.322	83.19	94.87	3.15	6.92	114.18	113.8	113.8	111.6	0.113	112.8
CAGrad+GraB	0.111	0.312	82.49	94.71	2.96	6.77	113.89	113.7	110.4	111.8	0.108	112.1
CAGrad+JoGBa	0.110	0.304	82.38	94.49	2.92	6.49	113.22	113.5	110.2	111.6	0.104	**111.9**
Nash-MTL (Random)	0.102	0.248	82.95	81.89	2.42	5.38	74.50	75.02	75.10	74.16	0.093	62.0
Nash-MTL+FlipFlop	0.106	0.255	82.79	82.01	2.45	5.42	74.52	75.07	75.13	74.27	0.096	62.2
Nash-MTL+Random FlipFlop	0.097	0.254	82.53	81.47	2.42	5.29	74.41	75.08	75.07	74.22	0.094	61.6
Nash-MTL+GraB	0.099	0.252	82.64	81.68	2.38	5.31	74.43	74.94	75.05	74.13	0.091	61.7
Nash-MTL+JoGBa	0.094	0.231	82.24	80.73	2.29	5.24	74.37	74.84	75.03	74.05	0.087	**59.2**

Table 3: Per-iteration CPU time cost (in seconds) of the two key steps in JoGBa combined with different multi-objective optimization algorithms.

	NYUv2				QM9			
	MGDA	PCGrad	CAGrad	Nash-MTL	MGDA	PCGrad	CAGrad	Nash-MTL
Sample ordering	0.02	0.03	0.03	0.03	0.06	0.05	0.04	0.05
Model update	1.04	0.91	0.99	1.06	2.97	1.37	1.17	1.62

Table 4: Test performance (averaged over 3 random seeds) for three tasks on NYUv2 with different sample ordering methods for the proposed multi-ordering framework.

	Segmentation		Depth		Surface Normal					
					Angle Distance ↓		Within t° ↑			$\mathbf{\Delta m}\% \downarrow$
	mIoU ↑	Pix Acc ↑	Abs Err ↓	Rel Err ↓	Mean	Median	11.25	22.5	30	
MGDA+Random	30.48	59.77	0.6020	0.2555	24.13	19.22	29.51	57.11	69.58	1.31
MGDA+FlipFlop	29.47	57.90	0.6270	0.2755	24.88	19.45	29.18	55.88	68.36	1.58
MGDA+Random FlipFlop	30.52	59.81	0.6018	0.2556	24.11	19.16	29.52	57.23	69.56	1.28
MGDA+GraB	30.74	59.92	0.6011	0.2524	24.12	19.11	29.54	57.35	69.76	1.25
MGDA+JoGBa	31.02	60.21	0.6008	0.2508	24.08	19.08	29.55	57.47	70.03	**1.19**
PCGrad+Random	38.06	64.64	0.5550	0.2325	27.41	22.80	23.86	49.83	63.14	3.97
PCGrad+FlipFlop	37.74	64.63	0.5590	0.2285	26.84	22.19	23.96	49.30	62.94	3.89
PCGrad+Random FlipFlop	38.12	64.64	0.5570	0.2329	26.99	22.67	23.56	49.65	63.18	3.86
PCGrad+GraB	38.31	64.66	0.5552	0.2317	26.79	22.87	23.68	49.76	63.22	3.78
PCGrad+JoGBa	38.59	64.67	0.5545	0.2270	26.53	22.40	23.87	49.95	63.87	**3.56**
CAGrad+Random	39.79	65.49	0.5486	0.2250	26.31	21.58	25.61	52.36	65.58	0.20
CAGrad+FlipFlop	39.42	65.55	0.5437	0.2219	25.79	21.75	25.97	52.17	65.34	0.27
CAGrad+Random FlipFlop	39.85	65.73	0.5467	0.2226	26.14	21.46	25.62	52.24	65.62	0.17
CAGrad+GraB	39.91	66.09	0.5428	0.2214	25.79	21.44	25.64	52.26	65.44	0.18
CAGrad+JoGBa	40.42	66.08	0.5410	0.2205	25.52	21.50	26.04	52.43	65.73	**0.03**
Nash-MTL+Random	40.13	65.93	0.5261	0.2171	25.26	20.08	28.40	55.47	68.15	−4.04
Nash-MTL+FlipFlop	39.46	65.82	0.5313	0.2190	26.12	20.99	28.05	54.64	67.77	-3.88
Nash-MTL+Random FlipFlop	40.67	66.32	0.5184	0.2009	25.34	19.73	28.54	55.35	68.07	-4.16
Nash-MTL+GraB	40.84	66.51	0.5156	0.2087	25.26	19.45	28.62	55.37	68.11	-4.19
Nash-MTL+JoGBa	41.13	66.71	0.5112	0.2009	25.11	19.19	28.77	55.28	68.18	**-4.27**

4.4 Ablation Study

Besides using the balancing routine as in Algorithm 1, other data ordering methods (e.g., those mentioned in Section 3.1) may also be used to obtain sample orders for different objectives. We use the same NYUv2 data set and training setup as in Section 4.1. and consider the following sample ordering methods for comparison: (i) Random reshuffling (Random), (ii) FlipFlop, which creates the new order π^m_{t+1} by reversing the previous order for each objective, i.e., $\pi^m_{t+1}(k) = \pi^m_t(K+1-k)$.

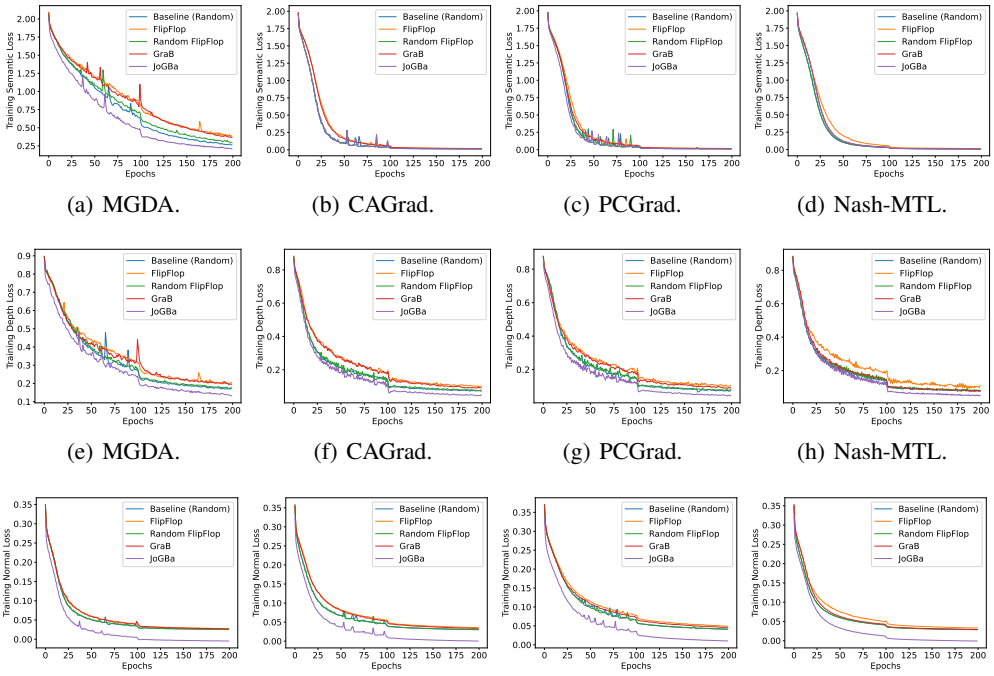

(a) MGDA. (b) CAGrad. (c) PCGrad. (d) Nash-MTL.

(e) MGDA. (f) CAGrad. (g) PCGrad. (h) Nash-MTL.

(i) MGDA. (j) CAGrad. (k) PCGrad. (l) Nash-MTL.

Figure 4: Training loss (objective values) of different tasks on NYUv2 data with different data ordering methods for the proposed multi-ordering framework. Top: Loss on the semantic segmentation task (semantic loss). Middle: Loss on the depth estimation task (depth loss). Bottom: Loss on the surface normal prediction task (normal loss).

(iii) Random FlipFlop (Random FF), the combination of random reshuffling and FlipFlop, and (iv) GraB (Lu et al., 2022), which applies GraB to all objectives separately.

Figure 4 compares the convergence curves of different sample ordering methods. Similar to Figure 2, the influence of sample orders on the convergence rate is generally different for different objectives. The surface normal prediction task is more influenced by different sample ordering methods than other two tasks. FlipFlop and GraB generally achieves worse performance than other methods, while JoGBa is the only one that can consistently outperforms existing baseline with random ordering.

Table 4 compares the testing performance of different data ordering combined with different multi-objective optimization methods. FlipFlop generally performs worse than other methods as it only reverse the sample ordering after each epoch. Both Random FlipFlop and GraB improve upon the standard random baseline, but their performance is still worse than the proposed method JoGBa, which demonstrate the effectiveness of joint sample ordering in multi-objective optimization.

5 Conclusion

In this paper, we propose a novel sample ordering framework for multi-objective optimization. The proposed framework determines sample orders for each objective by performing online vector balancing with the gradients on different objectives. It can be seamlessly combined with existing multi-objective optimization methods. Theoretical results demonstrate that the proposed method improves upon the baseline of random ordering with faster convergence. Empirical results on different multi-objective optimization problems demonstrate that the proposed method achieves faster convergence and better performance than the other data ordering methods.

Acknowledgments

This research is supported in part by the Research Grants Council of the Hong Kong Special Administrative Region (Grants 16200021, 16202523 and C7004-22G-1).

REFERENCES

Hao Ban and Kaiyi Ji. Fair resource allocation in multi-task learning. In Ruslan Salakhutdinov, Zico Kolter, Katherine Heller, Adrian Weller, Nuria Oliver, Jonathan Scarlett, and Felix Berkenkamp (eds.), *Proceedings of the 41st International Conference on Machine Learning*, pp. 2715–2731, 2024.

Dimitri P. Bertsekas. Incremental Gradient, Subgradient, and Proximal Methods for Convex Optimization: A Survey. In *Optimization for Machine Learning*. The MIT Press, 2011.

Jaeyoung Cha, Jaewook Lee, and Chulhee Yun. Tighter lower bounds for shuffling SGD: Random permutations and beyond. In *International Conference on Machine Learning*, 2023.

Lisha Chen, Heshan Fernando, Yiming Ying, and Tianyi Chen. Three-Way Trade-Off in Multi-Objective Learning: Optimization, Generalization and Conflict-Avoidance. *Journal of Machine Learning Research*, 25(193):1–53, 2024.

Zhao Chen, Vijay Badrinarayanan, Chen-Yu Lee, and Andrew Rabinovich. Gradnorm: Gradient normalization for adaptive loss balancing in deep multitask networks. July 2018.

Jean-Antoine Désidéri. Multiple-gradient Descent Algorithm (MGDA) for Multi-objective Optimization. *Comptes Rendus Mathematique*, 350(5-6), 2012.

Heshan Fernando, Han Shen, Miao Liu, Subhajit Chaudhury, Keerthiram Murugesan, and Tianyi Chen. Mitigating gradient bias in multi-objective learning: A provably convergent stochastic approach. 2023.

Jörg Fliege, A Ismael F Vaz, and Luís Nunes Vicente. Complexity of Gradient Descent for Multiobjective Optimization. *Optimization Methods and Software*, 34(5):949–959, 2019.

Justin Gilmer, Samuel S Schoenholz, Patrick F Riley, Oriol Vinyals, and George E Dahl. Neural message passing for quantum chemistry. In *International conference on machine learning*, pp. 1263–1272. PMLR, 2017.

Michelle Guo, Albert Haque, De-An Huang, Serena Yeung, and Li Fei-Fei. Dynamic task prioritization for multitask learning. In *Proceedings of the European conference on computer vision*, Munich, Germany, July 2018.

Mert Gürbüzbalaban, Asuman E. Ozdaglar, and Pablo A. Parrilo. Convergence rate of incremental gradient and incremental Newton methods. *SIAM Journal on Optimization*, 29(4):2542–2565, 2019.

A Kendall, Y Gal, and R Cipolla. Multi-task learning using uncertainty to weigh losses for scene geometry and semantics. *arXiv preprint:1705.07115*, 2017.

Diederik P. Kingma and Jimmy Ba. Adam: A method for stochastic optimization. In *International Conference on Learning Representations*, 2015.

Vitaly Kurin, Alessandro De Palma, Ilya Kostrikov, Shimon Whiteson, and M. Pawan Kumar. In defense of the unitary scalarization for deep multi-task learning. In *Advances in Neural Information Processing Systems*, 2022.

Bo Liu, Xingchao Liu, Xiaojie Jin, Peter Stone, and Qiang Liu. Conflict-Averse Gradient Descent for Multi-task Learning. December 2021.

Shikun Liu, Edward Johns, and Andrew J. Davison. End-to-end multi-task learning with attention. In *Proceedings of the IEEE/CVF Conference on Computer Vision and Pattern Recognition (CVPR)*, June 2019.

Suyun Liu and Luis Nunes Vicente. The Stochastic Multi-gradient Algorithm for Multi-objective Optimization and its Application to Supervised Machine Learning. *Annals of Operations Research*, pp. 1–30, 2021.

Yucheng Lu, Si Yi Meng, and Christopher De Sa. A General Analysis of Example-Selection for Stochastic Gradient Descent. In *International Conference on Learning Representations*, 2021.

Yucheng Lu, Wentao Guo, and Christopher M De Sa. Grab: Finding provably better data permutations than random reshuffling. *Advances in Neural Information Processing Systems*, 35: 8969–8981, 2022.

Kristof Van Moffaert and Ann Nowé. Multi-objective reinforcement learning using sets of pareto dominating policies. *Journal of Machine Learning Research*, 15(107):3663–3692, 2014.

Amirkeivan Mohtashami, Sebastian Stich, and Martin Jaggi. Characterizing & finding good data orderings for fast convergence of sequential gradient methods. *arXiv preprint arXiv:2202.01838*, 2022.

Michinari Momma, Chaosheng Dong, and Jia Liu. A multi-objective/multi-task learning framework induced by pareto stationarity. pp. 15895–15907, 2022.

Aviv Navon, Aviv Shamsian, Idan Achituve, Haggai Maron, Kenji Kawaguchi, Gal Chechik, and Ethan Fetaya. Multi-Task Learning as a Bargaining Game. In *Proceedings of the 39th International Conference on Machine Learning*, pp. 16428–16446. PMLR, June 2022.

Shashank Rajput, Kangwook Lee, and Dimitris Papailiopoulos. Permutation-based sgd: Is random optimal? *arXiv preprint arXiv:2102.09718*, 2021.

Raghunathan Ramakrishnan, Pavlo O. Dral, Matthias Rupp, and O. Anatole Von Lilienfeld. Quantum chemistry structures and properties of 134 kilo molecules. *Scientific Data*, 1:140022, 2014.

Benjamin Recht and Christopher Ré. Toward a noncommutative arithmetic-geometric mean inequality: Conjectures, case-studies, and consequences. In *Conference on Learning Theory*, volume 23, pp. 11.1–11.24, 2012.

Ozan Sener and Vladlen Koltun. Multi-task learning as multi-objective optimization. December 2018.

Nathan Silberman, Derek Hoiem, Pushmeet Kohli, and Rob Fergus. Indoor segmentation and support inference from rgbd images. In *European Conference on Computer Vision*, 2012.

Joel Spencer. Balancing games. *Journal of Combinatorial Theory, Series B*, 23(1):68–74, 1977.

Hiroki Tanabe, Ellen H. Fukuda, and Nobuo Yamashita. Proximal gradient methods for multiobjective optimization and their applications. *Computational Optimization and Applications*, 72(2): 339–361, 2019.

Max Welling. Herding dynamical weights to learn. In *Proceedings of the 26th Annual International Conference on Machine Learning*, pp. 1121–1128, 2009.

Derrick Xin, Behrooz Ghorbani, Justin Gilmer, Ankush Garg, and Orhan Firat. Do current multi-task optimization methods in deep learning even help? In *Advances in Neural Information Processing Systems*, 2022.

Feiyang Ye, Baijiong Lin, Zhixiong Yue, Pengxin Guo, Qiao Xiao, and Yu Zhang. Multi-objective meta learning. volume 34, pp. 21338–21351, 2021.

Bicheng Ying, Kun Yuan, Stefan Vlaski, and Ali H. Sayed. On the performance of random reshuffling in stochastic learning. In *2017 Information Theory and Applications Workshop (ITA)*, pp. 1–5. IEEE, 2017.

Tianhe Yu, Saurabh Kumar, Abhishek Gupta, Sergey Levine, Karol Hausman, and Chelsea Finn. Gradient surgery for multi-task learning. December 2020.

Muhammad Bilal Zafar, Isabel Valera, Manuel Gomez Rogriguez, and Krishna P Gummadi. Fairness constraints: Mechanisms for fair classification. pp. 962–970, 2017.

Shiji Zhou, Wenpeng Zhang, Jiyan Jiang, Wenliang Zhong, Jinjie Gu, and Wenwu Zhu. On the convergence of stochastic multi-objective gradient manipulation and beyond. volume 35, pp. 38103–38115, December 2022.

A PROOFS

A.1 PROOF OF THEOREM 3.6

Theorem 3.6. By the F_1-smoothness of $\mathcal{L}(\boldsymbol{w})\lambda$ for all $\lambda \in \Delta^M$, we have

$$\mathcal{L}(\boldsymbol{w}_{t+1})\lambda - \mathcal{L}(\boldsymbol{w}_t)\lambda \leq \langle \nabla \mathcal{L}(\boldsymbol{w})\lambda, \boldsymbol{w}_{t+1} - \boldsymbol{w}_t \rangle + \frac{F_1}{2}\|\boldsymbol{w}_{t+1} - \boldsymbol{w}_t\|^2 \tag{3}$$

where $\boldsymbol{w}_{t+1} - \boldsymbol{w}_t = \alpha_t \nabla \mathcal{L}(\boldsymbol{w}_t)\lambda_t^*$, s.t. $\lambda_t^* \in \arg\min_{\lambda \in \Delta^M} \|\nabla \mathcal{L}(\boldsymbol{w}_t)\lambda\|^2$. For notation simplicity, we define $Q_t = \nabla \mathcal{L}(\boldsymbol{w}_t)$, and $\lambda_{Q_t}^* = \arg\min_{\lambda \in \Delta^M} \|\nabla \mathcal{L}(\boldsymbol{w}_t)\lambda\|$. Then we have:

$$\mathcal{L}(\boldsymbol{w}_{t+1})\lambda - \mathcal{L}(\boldsymbol{w}_t)\lambda \leq -\alpha_t \langle \nabla \mathcal{L}(\boldsymbol{w}_t)\lambda, Q_t \lambda_{Q_t}^* \rangle + \frac{F_1}{2}\alpha_t^2 \|Q_t \lambda_{Q_t}^*\|^2. \tag{4}$$

The inner product term can be bounded as

$$-\langle \nabla \mathcal{L}(\boldsymbol{w}_t)\lambda, Q_t \lambda_{Q_t}^* \rangle = \langle \nabla \mathcal{L}(\boldsymbol{w}_t)\lambda, \nabla \mathcal{L}(\boldsymbol{w}_t)\lambda_t^*(\boldsymbol{w}_t) - Q_t \lambda_{Q_t}^* \rangle - \langle \nabla \mathcal{L}(\boldsymbol{w}_t)\lambda, \nabla \mathcal{L}(\boldsymbol{w}_t)\lambda_t^*(\boldsymbol{w}_t) \rangle \tag{5}$$

$$\overset{(a)}{\leq} \langle \nabla \mathcal{L}(\boldsymbol{w}_t)\lambda, \nabla \mathcal{L}(\boldsymbol{w}_t)\lambda_t^*(\boldsymbol{w}_t) - Q_t \lambda_{Q_t}^* \rangle - \|\nabla \mathcal{L}(\boldsymbol{w}_t)\lambda_t^*(\boldsymbol{w}_t)\|^2 \tag{6}$$

$$\leq F \|\nabla \mathcal{L}(\boldsymbol{w}_t)\lambda_t^*(\boldsymbol{w}_t) - Q_t \lambda_{Q_t}^*\| - \|\nabla \mathcal{L}(\boldsymbol{w}_t)\lambda_t^*(\boldsymbol{w}_t)\|^2 \tag{7}$$

$$\overset{(b)}{\leq} 2F^{\frac{3}{2}} \|Q_t - \nabla \mathcal{L}(\boldsymbol{w}_t)\|^{\frac{1}{2}} - \|\nabla \mathcal{L}(\boldsymbol{w}_t)\lambda_t^*(\boldsymbol{w}_t)\|^2 \tag{8}$$

where (a) follows from (18) in Lemma A.3, (b) follows from Lemma A.4. Plugging (8) into (4), taking expectations on both sides and rearranging yield

$$\alpha_t \mathbb{E}_A[\|\nabla \mathcal{L}(\boldsymbol{w}_t)\lambda_t^*(\boldsymbol{w}_t)\|^2] \leq \mathbb{E}_A[\mathcal{L}(\boldsymbol{w}_t) - \mathcal{L}(\boldsymbol{w}_{t+1})]\lambda + 2F^{\frac{3}{2}}\alpha_t \mathbb{E}_A[\|Q_t - \nabla \mathcal{L}(\boldsymbol{w}_t)\|^{\frac{1}{2}}] + \frac{F_1}{2}(F^2 + \sigma^2)\alpha_t^2.$$

For all $t \in [T]$, plugging in $\alpha_t = \alpha$, and taking the telescope sum on both sides of the last inequality yield

$$\frac{1}{T}\sum_{t=1}^{T} \mathbb{E}_A[\|\nabla \mathcal{L}(\boldsymbol{w}_t)\lambda_t^*(x_t)\|^2] \tag{9}$$

$$\leq \frac{1}{\alpha T}\mathbb{E}_A[\mathcal{L}(\boldsymbol{w}_t) - \mathcal{L}(\boldsymbol{w}_{t+1})]\lambda + 2\ell_f^{\frac{3}{2}} \frac{1}{T}\sum_{t=1}^{T} \mathbb{E}_A[\|Q_t - \nabla \mathcal{L}(\boldsymbol{w}_t)\|^{\frac{1}{2}}] + \frac{F_1}{2}(F^2 + \sigma^2)\alpha \tag{10}$$

$$\leq \frac{1}{\alpha T}\mathbb{E}_A[\mathcal{L}(\boldsymbol{w}_t) - \mathcal{L}(\boldsymbol{w}_{t+1})]\lambda + 2\ell_f^{\frac{3}{2}} \Big(\frac{1}{T}\sum_{t=1}^{T} \mathbb{E}_A[\|Q_t - \nabla \mathcal{L}(\boldsymbol{w}_t)\|^2]\Big)^{\frac{1}{4}} + \frac{F_1}{2}(F^2 + \sigma^2)\alpha. \tag{11}$$

By increasing the batch size during optimization with a batch size of $\mathcal{O}(t)$, it holds that

$$\frac{1}{T}\sum_{t=1}^{T} \mathbb{E}_A[\|Q_t - \nabla \mathcal{L}(\boldsymbol{w}_t)\|^2] \leq \frac{1}{T}\sum_{t=1}^{T} \frac{\sigma^2}{t} \leq \frac{\sigma^2(1 + \log(T))}{T} \tag{12}$$

Plugging (12) back into (11), its optimization error is given by:

$$\begin{aligned}
\mathbb{E}_A\Big[\min_{t \in [T], \lambda \in \Delta^M} \|\nabla \mathcal{L}(\boldsymbol{w}_t)\lambda\|^2\Big] &\leq \frac{1}{T}\sum_{t=1}^{T} \mathbb{E}_A[\|\nabla \mathcal{L}(\boldsymbol{w}_t)\lambda_t^*(\boldsymbol{w}_t)\|^2] \\
&= \frac{\sigma^2(1 + \log(T))}{T} + \frac{\mathbb{E}_A[\mathcal{L}(\boldsymbol{w}_t) - \mathcal{L}(\boldsymbol{w}_{T+1})]\lambda}{\alpha K T} + \frac{F_1}{2}(F^2 + \sigma^2)\alpha \\
&\leq \frac{\sigma^2(1 + \log(T))}{T} + \frac{\Delta}{\alpha K T} + \frac{F_1}{2}(F^2 + \sigma^2)\alpha
\end{aligned} \tag{13}$$

where the last inequality uses the definition of $\Delta = \max_{\lambda \in \Delta^M} \mathcal{L}(\boldsymbol{w}_0)\lambda - \min_{\boldsymbol{w} \in \mathbb{R}^d, \lambda \in \Delta^M} \mathcal{L}(\boldsymbol{w})\lambda$. Then setting $\alpha = \sqrt{\frac{2\Delta}{F_1(F^2+\sigma^2)KT}}$, we will have:

$$\mathbb{E}_A\Big[\min_{t \in [T], \lambda \in \Delta^M} \|\nabla \mathcal{L}(\boldsymbol{w}_t)\lambda\|^2\Big] \leq \sqrt{\frac{2F_1\Delta(F^2 + \sigma^2)}{KT}} + \frac{\sigma^2(1 + \log(T))}{T},$$

which concludes our proof. □

A.2 PROOF FOR PROPOSITION 3.8

Proof. The proof follows directly by using Assumption 3.3 in Assumption 3.7 for each $\|\nabla \ell_i(\boldsymbol{w})\|_\infty \leq F$. □

A.3 PROOF OF THEOREM 3.9

Proof. From Lemma A.1 in Appendix A.5, we have

$$\frac{1}{T}\sum_{t=0}^{T-1} \min_{\lambda \in \Delta^M} \|\nabla \mathcal{L}(\boldsymbol{w}_t^{(1)})\lambda\|^2 \leq \frac{2\Delta}{\alpha K T} + \frac{2F_1^2}{T}\sum_{t=0}^{T-1} \max_k \left\|\boldsymbol{w}_t^{(k)} - \boldsymbol{w}_t^{(1)}\right\|_\infty^2 + \frac{\alpha^2 F_1(F^2+\sigma^2)}{2}.$$

On the other hand, from Lemma A.2, we obtain

$$\sum_{t=0}^{T-1} \Delta_t^2 \leq 120\alpha^2 K^2\sigma^2 + 64\alpha^2 A^2\sigma^2 T + 48\alpha^2 K^2 \sum_{t=0}^{T-1} \max_k \|\nabla \mathcal{L}(\boldsymbol{w}_t^{(k)})\lambda\|_\infty^2.$$

Combining them together gives us,

$$\begin{aligned}
\frac{1}{T}\sum_{t=0}^{T-1} \min_{\lambda \in \Delta^M} \|\nabla \mathcal{L}(\boldsymbol{w}_t^{(1)})\lambda\|^2 \leq & \frac{2\Delta}{\alpha K T} \\
& + \frac{F_1^2}{T}\left(120\alpha^2 K^2\sigma^2 + 64\alpha^2 A^2\sigma^2 T + 48\alpha^2 K^2 \sum_{t=0}^{T-1} \max_k \|\nabla \mathcal{L}(\boldsymbol{w}_t^{(k)})\lambda\|_\infty^2\right) \\
& + + \frac{\alpha^2 F_1(F^2+\sigma^2)}{2} \\
\leq & \frac{2\Delta}{\alpha K T} + \frac{120\alpha^2 F_1^2 K^2\sigma^2}{T} + 64\alpha^2 A^2 F_1^2\sigma^2 \\
& + \frac{48\alpha^2 K^2 F_1^2}{T}\sum_{t=0}^{T-1} \max_k \|\nabla \mathcal{L}(\boldsymbol{w}_t^{(k)})\lambda\|_\infty^2 + \frac{\alpha^2 F_1(F^2+\sigma^2)}{2}.
\end{aligned}$$

Note that for any $\boldsymbol{x} \in \mathbb{R}^d$, $\|\boldsymbol{x}\|_\infty \leq \|\boldsymbol{x}\|_2$, so the last term can by bounded by its ℓ_2-norm. Moving it to the left side of the inequality gives us

$$\begin{aligned}
\frac{1 - 48\alpha^2 K^2 F_1^2}{T}\sum_{t=0}^{T-1} \min_{\lambda \in \Delta^M} \|\nabla \mathcal{L}(\boldsymbol{w}_t^{(1)})\lambda\|^2 \leq & \frac{2\Delta}{\alpha K T} + \frac{120\alpha^2 F_1^2 K^2\sigma^2}{T} + 64\alpha^2 A^2 F_1^2\sigma^2 \\
& + \frac{\alpha^2 F_1(F^2+\sigma^2)}{2}.
\end{aligned}$$

Finally, we set the value of α as follows:

$$\alpha = \min\left\{\sqrt[3]{\frac{\Delta}{32KA^2\sigma^2F_1^2T}}, \frac{1}{KF}, \frac{1}{26(K+A)F_1}\right\},$$

and we finally obtain

$$\frac{1}{T}\sum_{t=0}^{T-1} \min_{\lambda \in \Delta^M} \|\nabla \mathcal{L}(\boldsymbol{w}_t^{(1)})\lambda\|^2 \leq 11\sqrt[3]{\frac{A^2F_1^2\Delta^2(F^2+\sigma^2)}{K^2T^2}} + \frac{\sigma^2}{T} + \frac{65\Delta(F+F_1)}{T} + \frac{8\Delta A F_1}{KT},$$

which concludes our proof. □

A.4 PROOF FOR PROPOSITION 3.10

Proof. Similar to Proposition 3.8, the proof follows directly by using Assumption 3.3 in Assumption 3.7 for each $\|\nabla \ell_i(\boldsymbol{w})\|_\infty \leq F$, and repeated for M obejctives. □

A.5 TECHNICAL LEMMAS

Lemma A.1. *In Algorithm 1, if $\alpha KF < 1$ holds and Assumption 3.3 and 3.4 hold, then*

$$\frac{1}{T}\sum_{t=0}^{T-1}\min_{\lambda\in\Delta^M}\|\nabla\mathcal{L}(\boldsymbol{w}_t^{(1)})\lambda\|^2 \leq \frac{2\Delta}{\alpha KT} + \frac{2F_1^2}{T}\sum_{t=0}^{T-1}\max_k\left\|\boldsymbol{w}_t^{(k)} - \boldsymbol{w}_t^{(1)}\right\|_\infty^2 + \frac{\alpha^2 F_1(F^2+\sigma^2)}{2}.$$

Proof. Note that the update can be written as

$$\boldsymbol{w}_{t+1}^{(1)} = \boldsymbol{w}_t^{(1)} - \alpha\sum_{k=1}^K\sum_{m=1}^M \lambda_{k,m}\nabla\ell_m(\boldsymbol{w}_t^{(k)};\xi_{\pi_k^m(t)}).$$

By the Taylor Theorem, for all the $t = 0, \cdots, T-1$,

$$\begin{aligned}
\mathcal{L}(\boldsymbol{w}_{t+1}^{(1)})\lambda \leq& \mathcal{L}(\boldsymbol{w}_t^{(1)})\lambda + \langle\nabla\mathcal{L}(x_t)\lambda, \boldsymbol{w}_{t+1}^{(1)} - \boldsymbol{w}_t^{(1)}\rangle + \frac{F_1}{2}\|\boldsymbol{w}_{t+1}^{(1)} - \boldsymbol{w}_t^{(1)}\|^2\\
\leq& \mathcal{L}(\boldsymbol{w}_t^{(1)})\lambda - \alpha K\mathbb{E}\left\langle\nabla\mathcal{L}(\boldsymbol{w}_t)\lambda, \frac{1}{K}\sum_{k=1}^K\sum_{m=1}^M\lambda_{i,k}\nabla\ell_i(\boldsymbol{w}_t^{(k)};\xi_{\pi_t^m(t)})\right\rangle\\
&+ \frac{\alpha^2K^2F_1}{2}\mathbb{E}\left\|\frac{1}{K}\sum_{k=1}^K\sum_{m=1}^M\lambda_{i,k}\nabla\ell_i(\boldsymbol{w}_t^{(k)};\xi_{\pi_i(t)})\right\|^2\\
=& \mathcal{L}(\boldsymbol{w}_t^{(1)})\lambda - \frac{\alpha K}{2}\|\nabla\mathcal{L}(\boldsymbol{w}_t^{(1)})\lambda\|^2 - \frac{\alpha K}{2}\|\frac{1}{K}\sum_{k=1}^K\sum_{m=1}^M\lambda_{i,k}\nabla\ell_i(\boldsymbol{w}_t^{(k)};\xi_{\sigma_k(t)})\|^2\\
&+ \frac{\alpha K}{2}\|\nabla\mathcal{L}(\boldsymbol{w}_t^{(1)})\lambda - \frac{1}{K}\sum_{k=1}^K\sum_{m=1}^M\lambda_{i,k}\nabla\ell_i(\boldsymbol{w}_t^{(k)};\xi_{\sigma_k(t)})\|^2 + \frac{\alpha^2K^2F_1}{2}\mathbb{E}\left\|\frac{1}{K}\sum_{k=1}^K\sum_{i=1}^m\lambda_{i,k}\nabla\ell_i(\boldsymbol{w}_k^{(t)};\xi_{\sigma_k(t)})\right\|^2\\
\leq& \mathcal{L}(\boldsymbol{w}_t^{(1)})\lambda - \frac{\alpha K}{2}\|\nabla\mathcal{L}(\boldsymbol{w}_t^{(1)})\lambda\|^2 + \frac{\alpha K}{2}\|\nabla\mathcal{L}(\boldsymbol{w}_t^{(1)})\lambda - \frac{1}{K}\sum_{k=1}^K\sum_{m=1}^M\lambda_{i,k}\nabla\ell_i(\boldsymbol{w}_t^{(k)};\xi_{\sigma_k(t)})\|^2\\
&+ \frac{\alpha^2F_1(F^2+\sigma^2)}{2}
\end{aligned}$$

In the second step, we apply $-\langle\boldsymbol{a},\boldsymbol{b}\rangle = -\frac{1}{2}\|\boldsymbol{a}\|^2 - \frac{1}{2}\|\boldsymbol{b}\|^2 + \frac{1}{2}\|\boldsymbol{a}-\boldsymbol{b}\|^2, \forall\boldsymbol{a},\boldsymbol{b}$. In the third step, we use the condition that $\alpha nL < 1$. Expanding the last term using Assumption 3.4, we get

$$\begin{aligned}
\|\nabla\mathcal{L}(\boldsymbol{w}_t^{(1)})\lambda - \frac{1}{K}\sum_{k=1}^K\sum_{m=1}^M\lambda_{m,k,t}\nabla\ell_m(\boldsymbol{w}_t^{(k)};\xi_{\sigma_t^m(k)})\|^2 =& \left\|\frac{1}{K}\sum_{k=1}^K\nabla\mathcal{L}(\boldsymbol{w}_t^{(1)})\lambda - \frac{1}{K}\sum_{k=1}^K\sum_{m=1}^M\lambda_{m,k,t}\nabla\ell_m(\boldsymbol{w}_t^{(k)};\xi_{\sigma_t^m(k)})\right\|^2\\
\leq& \frac{1}{K}\sum_{k=1}^K\left\|\nabla\mathcal{L}(\boldsymbol{w}_t^{(1)})\lambda - \nabla\mathcal{L}(\boldsymbol{w}_t^{(k)})\lambda\right\|^2\\
\leq& \frac{1}{K}\sum_{k=1}^K F_1^2\left\|\boldsymbol{w}_t^{(1)} - \boldsymbol{w}_t^{(k)}\right\|_\infty^2\\
\leq& F_1^2\Delta_k^2.
\end{aligned}$$

In the second step we apply the Jensen Inequality. Put it back, we obtain

$$\mathcal{L}(\boldsymbol{w}_{t+1}^{(1)})\lambda \leq \mathcal{L}(\boldsymbol{w}_t^{(1)})\lambda - \frac{\alpha K}{2}\left\|\nabla\mathcal{L}(\boldsymbol{w}_t^{(1)})\lambda\right\|^2 + \frac{\alpha K}{2}F_1^2\Delta_k^2 + \frac{\alpha^2F_1(F^2+\sigma^2)}{2}.$$

Finally, summing from $t = 0$ to $T-1$, and considering the definition $\Delta = \max_{\lambda\in\Delta^M}\mathcal{L}(\boldsymbol{w}_0)\lambda - \min_{\boldsymbol{w}\in\mathbb{R}^d,\lambda\in\Delta^M}\mathcal{L}(\boldsymbol{w})\lambda$, we will have:

$$\frac{1}{T}\sum_{t=0}^{T-1}\min_{\lambda\in\Delta^M}\|\nabla\mathcal{L}(\boldsymbol{w}_t^{(1)})\lambda\|^2 \leq \frac{2\Delta}{\alpha KT} + \frac{2F_1^2}{T}\sum_{t=0}^{T-1}\max_k\left\|\boldsymbol{w}_t^{(k)} - \boldsymbol{w}_t^{(1)}\right\|_\infty^2 + \frac{\alpha^2F_1(F^2+\sigma^2)}{2}.$$

That completes our proof. □

Lemma A.2. *In Algorithm 1, if the learning rate α fulfills*

$$\alpha \leq \min\left\{\frac{1}{32nL_\infty}, \frac{1}{16HL_2}\right\},$$

then the following inequalities hold:

$$\Delta_k \leq 2\alpha H\varsigma + (8\alpha nL_\infty + 4\alpha HL_2)\Delta_{k-1} + 2\alpha n\|\nabla\mathcal{L}(\boldsymbol{w}_k)\|_\infty, \forall k \geq 2$$

and,

$$\Delta_1^2 \leq 8\alpha^2 n^2\|\nabla\mathcal{L}(\boldsymbol{w}_1)\|_\infty^2 + 8\alpha^2 n^2\varsigma^2,$$

and finally,

$$\sum_{k=1}^K \Delta_k^2 \leq 16\alpha^2 n^2\varsigma^2 + 48\alpha^2 H^2\varsigma^2 K + 48\alpha^2 n^2\sum_{k=1}^K\|\nabla\mathcal{L}(\boldsymbol{w}_k)\|_\infty^2.$$

Proof. Without the loss of generality, for all the $m \in \{2, \cdots, n+1\}$ and all the $k \in \{2, \cdots, K\}$,

$$\begin{aligned}
\boldsymbol{w}_k^{(m)} =& \boldsymbol{w}_k - \alpha\sum_{t=1}^{m-1}\nabla f\left(\boldsymbol{w}_k^{(t)}; \boldsymbol{x}_{\sigma_k(t)}\right) \\
=& \boldsymbol{w}_k - \alpha\sum_{t=1}^{m-1}\nabla f\left(\boldsymbol{w}_{k-1}^{(\sigma_{k-1}^{-1}(\sigma_k(t)))}; \boldsymbol{x}_{\sigma_k(t)}\right) \\
& - \alpha\sum_{t=1}^{m-1}\left(\nabla f\left(\boldsymbol{w}_k^{(t)}; \boldsymbol{x}_{\sigma_k(t)}\right) - \nabla f\left(\boldsymbol{w}_{k-1}^{(\sigma_{k-1}^{-1}(\sigma_k(t)))}; \boldsymbol{x}_{\sigma_k(t)}\right)\right).
\end{aligned}$$

Now add and subtract

$$\alpha\sum_{t=1}^{m-1}\frac{1}{n}\sum_{s=1}^n\nabla f\left(\boldsymbol{w}_{k-1}^{(s)}; \boldsymbol{x}_{\sigma_{k-1}(s)}\right) = \frac{\alpha(m-1)}{n}\sum_{t=1}^n\nabla f\left(\boldsymbol{w}_{k-1}^{(t)}; \boldsymbol{x}_{\sigma_{k-1}(t)}\right),$$

which gives

$$\begin{aligned}
\boldsymbol{w}_k^{(m)} =& \boldsymbol{w}_k - \alpha\sum_{t=1}^{m-1}\left(\nabla f\left(\boldsymbol{w}_{k-1}^{(\sigma_{k-1}^{-1}(\sigma_k(t)))}; \boldsymbol{x}_{\sigma_k(t)}\right) - \frac{1}{n}\sum_{s=1}^n\nabla f\left(\boldsymbol{w}_{k-1}^{(s)}; \boldsymbol{x}_{\sigma_{k-1}(s)}\right)\right) \\
& - \frac{\alpha(m-1)}{n}\sum_{t=1}^n\nabla f\left(\boldsymbol{w}_{k-1}^{(t)}; \boldsymbol{x}_{\sigma_{k-1}(t)}\right) \\
& - \alpha\sum_{t=1}^{m-1}\left(\nabla f\left(\boldsymbol{w}_k^{(t)}; \boldsymbol{x}_{\sigma_k(t)}\right) - \nabla f\left(\boldsymbol{w}_{k-1}^{(\sigma_{k-1}^{-1}(\sigma_k(t)))}; \boldsymbol{x}_{\sigma_k(t)}\right)\right).
\end{aligned}$$

We further add and subtract

$$\frac{\alpha(m-1)}{K}\sum_{k=1}^K\nabla\mathcal{L}(\boldsymbol{w}_t; \boldsymbol{x}_{\sigma_{t-1}(k)}) = \alpha(m-1)\nabla\mathcal{L}(\boldsymbol{w}_k)$$

to arrive at

$$\begin{aligned}
\boldsymbol{w}_k^{(m)} =& \boldsymbol{w}_k - \alpha\sum_{t=1}^{m-1}\left(\nabla f\left(\boldsymbol{w}_{k-1}^{(\sigma_{k-1}^{-1}(\sigma_k(t)))}; \boldsymbol{x}_{\sigma_k(t)}\right) - \frac{1}{n}\sum_{s=1}^n\nabla f\left(\boldsymbol{w}_{k-1}^{(s)}; \boldsymbol{x}_{\sigma_{k-1}(s)}\right)\right) \\
& - \alpha(m-1)\nabla\mathcal{L}(\boldsymbol{w}_k) + \frac{\alpha(m-1)}{n}\sum_{t=1}^n\left(\nabla f\left(\boldsymbol{w}_k; \boldsymbol{x}_{\sigma_{k-1}(t)}\right) - \nabla f\left(\boldsymbol{w}_{k-1}^{(t)}; \boldsymbol{x}_{\sigma_{k-1}(t)}\right)\right) \\
& - \alpha\sum_{t=1}^{m-1}\left(\nabla f\left(\boldsymbol{w}_k^{(t)}; \boldsymbol{x}_{\sigma_k(t)}\right) - \nabla f\left(\boldsymbol{w}_{k-1}^{(\sigma_{k-1}^{-1}(\sigma_k(t)))}; \boldsymbol{x}_{\sigma_k(t)}\right)\right).
\end{aligned}$$

We can now re-arrange, take norms on both sides and apply the triangle inequality,

$$\begin{aligned}\left\|\boldsymbol{w}_k^{(m)} - \boldsymbol{w}_k\right\|_\infty \leq \alpha &\left\|\sum_{t=1}^{m-1}\left(\nabla f\left(\boldsymbol{w}_{k-1}^{(\sigma_{k-1}^{-1}(\sigma_k(t)))}; \boldsymbol{x}_{\sigma_k(t)}\right) - \frac{1}{n}\sum_{s=1}^{n}\nabla f\left(\boldsymbol{w}_{k-1}^{(s)}; \boldsymbol{x}_{\sigma_{k-1}(s)}\right)\right)\right\|_\infty \\ &+ \alpha(m-1)\|\nabla\mathcal{L}(\boldsymbol{w}_k)\|_\infty \\ &+ \frac{\alpha(m-1)}{n}\left\|\sum_{t=1}^{n}\left(\nabla f\left(\boldsymbol{w}_k; \boldsymbol{x}_{\sigma_{k-1}(t)}\right) - \nabla f\left(\boldsymbol{w}_{k-1}^{(t)}; \boldsymbol{x}_{\sigma_{k-1}(t)}\right)\right)\right\|_\infty \\ &+ \alpha\left\|\sum_{t=1}^{m-1}\left(\nabla f\left(\boldsymbol{w}_k^{(t)}; \boldsymbol{x}_{\sigma_k(t)}\right) - \nabla f\left(\boldsymbol{w}_{k-1}^{(\sigma_{k-1}^{-1}(\sigma_k(t)))}; \boldsymbol{x}_{\sigma_k(t)}\right)\right)\right\|_\infty. \quad (14)\end{aligned}$$

There are four different terms on the right hand side, we will apply the Assumption 3.7 on the first term, and Assumption 3.4 on the last two terms. First, for the first term,

$$\begin{aligned}&\left\|\nabla f\left(\boldsymbol{w}_{k-1}^{(\sigma_{k-1}^{-1}(\sigma_k(t)))}; \boldsymbol{x}_{\sigma_k(t)}\right) - \frac{1}{n}\sum_{s=1}^{n}\nabla f\left(\boldsymbol{w}_{k-1}^{(s)}; \boldsymbol{x}_{\sigma_{k-1}(s)}\right)\right\| \\ \leq &\left\|\nabla f\left(\boldsymbol{w}_{k-1}^{(\sigma_{k-1}^{-1}(\sigma_k(t)))}; \boldsymbol{x}_{\sigma_k(t)}\right) - \frac{1}{n}\sum_{s=1}^{n}\nabla f\left(\boldsymbol{w}_{k-1}^{(\sigma_{k-1}^{-1}(\sigma_k(t)))}; \boldsymbol{x}_{\sigma_{k-1}(s)}\right)\right\| \\ &+ \left\|\frac{1}{n}\sum_{s=1}^{n}\nabla f\left(\boldsymbol{w}_{k-1}^{(\sigma_{k-1}^{-1}(\sigma_k(t)))}; \boldsymbol{x}_{\sigma_{k-1}(s)}\right) - \frac{1}{n}\sum_{s=1}^{n}\nabla f\left(\boldsymbol{w}_{k-1}^{(s)}; \boldsymbol{x}_{\sigma_{k-1}(s)}\right)\right\| \\ \overset{\text{Assumption 3.4 and 3.5}}{\leq} &\varsigma + \sigma_i + \frac{L_2}{n}\sum_{s=1}^{n}\left\|\boldsymbol{w}_{k-1}^{(\sigma_{k-1}^{-1}(\sigma_k(t)))} - \boldsymbol{w}_{k-1}^{(s)}\right\|_\infty \\ \leq &\max_m \sigma_m + \frac{L_2}{n}\sum_{s=1}^{n}\left(\left\|\boldsymbol{w}_{k-1} - \boldsymbol{w}_{k-1}^{(\sigma_{k-1}^{-1}(\sigma_k(t)))}\right\|_\infty + \left\|\boldsymbol{w}_{k-1} - \boldsymbol{w}_{k-1}^{(s)}\right\|_\infty\right) \\ \leq &\max_m \sigma_m + 2L_2\Delta_{k-1}\end{aligned}$$

This implies if we denote

$$\boldsymbol{u}_t := \nabla\ell\left(\boldsymbol{w}_{k-1}^{\sigma_{k-1}^{-1}(\sigma_k(t))}; \boldsymbol{x}_{\sigma_k(t)}\right) - \frac{1}{n}\sum_{s=1}^{n}\nabla\mathcal{L}(\boldsymbol{w}_{k-1}^{(s)}; \boldsymbol{x}_{\sigma_{k-1}(s)})$$

We can now use assumption 3.7 to obtain a bound on the prefix sum

$$\left\|\sum_{t=1}^{m-1}\frac{\boldsymbol{u}_t}{\varsigma + \sigma_i + 2L_2\Delta_{k-1}}\right\|_\infty \leq A,$$

that is,

$$\left\|\sum_{t=1}^{m-1}\left(\nabla f\left(\boldsymbol{w}_{k-1}^{(\sigma_{k-1}^{-1}(\sigma_k(t)))}; \boldsymbol{x}_{\sigma_k(t)}\right) - \frac{1}{n}\sum_{s=1}^{n}\nabla f\left(\boldsymbol{w}_{k-1}^{(s)}; \boldsymbol{x}_{\sigma_{k-1}(s)}\right)\right)\right\|_\infty \leq A(\varsigma + \sigma_i + 2L_2\Delta_{k-1}).$$

Now we have a bound for the first term in Equation (14), we proceed to bound the last two terms where we apply Assumption 3.4. We can then rewrite Equation (14) into,

$$\begin{aligned}\left\|\boldsymbol{w}_k^{(m)} - \boldsymbol{w}_k\right\|_\infty \leq &\alpha A(\varsigma + \sigma_i + 2L_2\Delta_{k-1}) + \alpha(m-1)\|\nabla\mathcal{L}(\boldsymbol{w}_k)\|_\infty + \frac{\alpha L_\infty(m-1)}{n}\sum_{t=1}^{n}\left\|\boldsymbol{w}_k - \boldsymbol{w}_{k-1}^{(t)}\right\|_\infty \\ &+ \alpha L_\infty\sum_{t=1}^{m-1}\left\|\boldsymbol{w}_k^{(t)} - \boldsymbol{w}_{k-1}^{(\sigma_{k-1}^{-1}(\sigma_k(t)))}\right\|_\infty.\end{aligned}$$

Furthermore, applying the triangle inequality to the norms in the last two terms, we obtain

$$\left\|\boldsymbol{w}_{k-1}^{(t)} - \boldsymbol{w}_k\right\|_\infty = \left\|\boldsymbol{w}_{k-1}^{(t)} - \boldsymbol{w}_{k-1} + \boldsymbol{w}_{k-1} - \boldsymbol{w}_{k-1}^{(n+1)}\right\|_\infty \leq 2\Delta_{k-1}$$

and similarly,

$$\left\|\boldsymbol{w}_k^{(t)} - \boldsymbol{w}_{k-1}^{(\sigma_{k-1}^{-1}(\sigma_k(t)))}\right\|_\infty = \left\|\boldsymbol{w}_k^{(t)} - \boldsymbol{w}_k + \boldsymbol{w}_k - \boldsymbol{w}_{k-1} + \boldsymbol{w}_{k-1} - \boldsymbol{w}_{k-1}^{(\sigma_{k-1}^{-1}(\sigma_k(t)))}\right\|_\infty \leq \Delta_k + 2\Delta_{k-1}.$$

This gives us

$$\begin{aligned}\left\|\boldsymbol{w}_k^{(m)} - \boldsymbol{w}_k\right\|_\infty \leq& \alpha A(\varsigma + \sigma_i + 2L_2\Delta_{k-1}) + \alpha(m-1)\|\nabla\mathcal{L}(\boldsymbol{w}_k)\|_\infty + 2\alpha L_\infty(m-1)\Delta_{k-1} \\ &+ \alpha L_\infty(m-1)(2\Delta_{k-1} + \Delta_k) \\ \leq& \alpha A(\varsigma + \sigma_i + 2L_2\Delta_{k-1}) + \alpha(m-1)\|\nabla\mathcal{L}(\boldsymbol{w}_k)\|_\infty + \alpha L_\infty(m-1)(4\Delta_{k-1} + \Delta_k).\end{aligned} \tag{15}$$

Note that Equation (15) only holds with $k \in \{2, \cdots, K\}$ and $m \in \{2, \cdots, n+1\}$. We now discuss the boundary cases. Note that the bound of Equation (15) trivially holds with $m = 1$ for any k since the left hand side becomes zero. On the other hand, when $k = 1$, we have,

$$\begin{aligned}\boldsymbol{w}_1^{(m)} =& \boldsymbol{w}_1 - \alpha\sum_{t=1}^{m-1}\nabla f\left(\boldsymbol{w}_1^{(t)}; \boldsymbol{x}_{\sigma_1(t)}\right) \\ =& \boldsymbol{w}_1 - \alpha\sum_{t=1}^{m-1}\frac{1}{n}\sum_{s=1}^{n}\nabla f\left(\boldsymbol{w}_1; \boldsymbol{x}_{\sigma_1(s)}\right) + \alpha\sum_{t=1}^{m-1}\nabla f\left(\boldsymbol{w}_1^{(t)}; \boldsymbol{x}_{\sigma_1(t)}\right) - \alpha\sum_{t=1}^{m-1}\nabla f\left(\boldsymbol{w}_1; \boldsymbol{x}_{\sigma_1(t)}\right) \\ &+ \alpha\sum_{t=1}^{m-1}\nabla f\left(\boldsymbol{w}_1; \boldsymbol{x}_{\sigma_1(t)}\right) - \alpha\sum_{t=1}^{m-1}\frac{1}{n}\sum_{s=1}^{n}\nabla f\left(\boldsymbol{w}_1; \boldsymbol{x}_{\sigma_1(s)}\right),\end{aligned}$$

take norms and apply the triangle inequality, we obtain

$$\begin{aligned}\left\|\boldsymbol{w}_1^{(m)} - \boldsymbol{w}_1\right\|_\infty \leq& \alpha\left\|\sum_{t=1}^{m-1}\frac{1}{n}\sum_{s=1}^{n}\nabla f\left(\boldsymbol{w}_1; \boldsymbol{x}_{\sigma_1(s)}\right)\right\|_\infty + \alpha\left\|\sum_{t=1}^{m-1}\left(\nabla f\left(\boldsymbol{w}_1^{(t)}; \boldsymbol{x}_{\sigma_1(t)}\right) - \nabla f\left(\boldsymbol{w}_1; \boldsymbol{x}_{\sigma_1(s)}\right)\right)\right\|_\infty \\ &+ \alpha\left\|\sum_{t=1}^{m-1}\left(\nabla f\left(\boldsymbol{w}_1; \boldsymbol{x}_{\sigma_1(t)}\right) - \frac{1}{n}\sum_{s=1}^{n}\nabla f\left(\boldsymbol{w}_1; \boldsymbol{x}_{\sigma_1(s)}\right)\right)\right\|_\infty \\ \leq& \alpha(m-1)\|\nabla\mathcal{L}(\boldsymbol{w}_1)\|_\infty + \alpha(m-1)L_\infty\Delta_1 + \alpha(m-1)(\varsigma + \sigma_i) \\ \leq& \alpha n\|\nabla\mathcal{L}(\boldsymbol{w}_1)\|_\infty + \alpha nL_\infty\Delta_1 + \alpha n(\varsigma + \sigma_i).\end{aligned} \tag{16}$$

Now that we have the bounds for Δ_k, we next will sum them up. Taking a max over m on both side in Equation (15), this implies for all the $k \geq 2$,

$$\Delta_k \leq \alpha H(\varsigma + \sigma_i + 2L_2\Delta_{k-1}) + \alpha L_\infty n(4\Delta_{k-1} + \Delta_k) + \alpha n\|\nabla\mathcal{L}(\boldsymbol{w}_k)\|_\infty$$

as $m - 1 \leq n$. Considering the fact that $\alpha L_\infty n < 1/2$, we get

$$\Delta_k \leq 2\alpha H\varsigma + \sigma_i + (8\alpha nL_\infty + 4\alpha HL_2)\Delta_{k-1} + 2\alpha n\|\nabla\mathcal{L}(\boldsymbol{w}_k)\|_\infty.$$

This completes the proof of the first inequality in the lemma. Applying this recursively from any $k \geq 2$ to 2, this gives

$$\Delta_k \leq (8\alpha nL_\infty + 4\alpha HL_2)^{k-1}\Delta_1 + \sum_{i=1}^{\infty}(8\alpha nL_\infty + 4\alpha HL_2)^i\left(2\alpha H(\varsigma + \sigma_i) + 2\alpha n\|\nabla\mathcal{L}(\boldsymbol{w}_k)\|_\infty\right).$$

Applying the learning rate conditions that $32\alpha nL_\infty \leq 1$ and $16\alpha HL_2 \leq 1$, we obtain

$$\Delta_k \leq \left(\frac{1}{2}\right)^{k-1}\Delta_1 + 4\alpha H(\varsigma + \sigma_i) + 4\alpha n\|\nabla\mathcal{L}(\boldsymbol{w}_k)\|_\infty.$$

Square on both sides,

$$\Delta_k^2 \leq 3\left(\frac{1}{4}\right)^{k-1}\Delta_1^2 + 48\alpha^2H^2(\varsigma + \sigma_i)^2 + 48\alpha^2n^2\|\nabla\mathcal{L}(\boldsymbol{w}_k)\|_\infty^2.$$

We can apply the similar trick to Equation (16) and get

$$\Delta_1^2 \leq 8\alpha^2 n^2 \|\nabla \mathcal{L}(\boldsymbol{w}_1)\|_\infty^2 + 8\alpha^2 n^2 (\varsigma + \sigma_i)^2.$$

This completes the proof of the second inequality in the lemma. Summing from $k = 1$ to K, we will get

$$\begin{aligned}
\sum_{k=1}^K \Delta_k^2 =& \Delta_1^2 + \sum_{k=2}^K \Delta_k^2 \\
=& \Delta_1^2 + 3\Delta_1^2 \sum_{k=2}^K \left(\frac{1}{4}\right)^{k-1} + 48\alpha^2 H^2 (\varsigma + \sigma_i)^2 (K-1) + 48\alpha^2 n^2 \sum_{k=2}^K \|\nabla \mathcal{L}(\boldsymbol{w}_k)\|_\infty^2 \\
\leq& \Delta_1^2 + 3\Delta_1^2 \sum_{k=1}^\infty \left(\frac{1}{4}\right)^{k} + 48\alpha^2 H^2 (\varsigma + \sigma_i)^2 (K-1) + 48\alpha^2 n^2 \sum_{k=2}^K \|\nabla \mathcal{L}(\boldsymbol{w}_k)\|_\infty^2 \\
\leq& 16\alpha^2 n^2 \|\nabla \mathcal{L}(\boldsymbol{w}_1)\|_\infty^2 + 16\alpha^2 n^2 (\varsigma + \sigma_i) 2 + 48\alpha^2 H^2 (\varsigma + \sigma_i)^2 (K-1) + 48\alpha^2 n^2 \sum_{k=2}^K \|\nabla \mathcal{L}(\boldsymbol{w}_k)\|_\infty^2 \\
\leq& 16\alpha^2 n^2 (\varsigma + \sigma_i)^2 + 48\alpha^2 H^2 (\varsigma + \sigma_i)^2 K + 48\alpha^2 n^2 \sum_{k=1}^K \|\nabla \mathcal{L}(\boldsymbol{w}_k)\|_\infty^2.
\end{aligned}$$

That completes the third inequality, and we have finished proving all three inequalities. □

Lemma A.3 ((Chen et al., 2024)). *Given $Q \in \mathbb{R}^{d\times M}$, recall $\lambda^*_{Q,\rho}$ with $\rho \geq 0$ is defined as*

$$\lambda^*_{Q,\rho} \in \arg\min_{\lambda \in \Delta^M} \|Q\lambda\|^2 + \rho\|\lambda\|^2. \tag{17}$$

Then, for any $\lambda \in \Delta^M$, it holds that

$$\langle Q\lambda^*_{Q,\rho}, Q\lambda\rangle \geq \|Q\lambda^*_{Q,\rho}\|^2 - \rho, \tag{18}$$

$$\text{and } \|Q\lambda - Q\lambda^*_{Q,\rho}\|^2 \leq \|Q\lambda\|^2 - \|Q\lambda^*_{Q,\rho}\|^2 + 2\rho. \tag{19}$$

Proof. By the first order optimality condition for equation 17 , for any $\lambda \in \Delta^M$, we have

$$\langle Q^\top Q\lambda^*_{Q,\rho}, \lambda - \lambda^*_{Q,\rho}\rangle \geq -\rho. \tag{20}$$

By rearranging the above inequality, we obtain

$$\langle Q\lambda^*_{Q,\rho}, Q\lambda\rangle \geq \|Q\lambda^*_{Q,\rho}\|^2 - \rho, \tag{21}$$

which is precisely the first inequality in the claim. Furthermore, we can also have

$$\begin{aligned}
\|Q\lambda - Q\lambda^*_{Q,\rho}\|^2 &= \|Q\lambda\|^2 + \|Q\lambda^*_{Q,\rho}\|^2 - 2\langle Q\lambda^*_{Q,\rho}, Q\lambda\rangle \\
&\leq \|Q\lambda\|^2 + \|Q\lambda^*_{Q,\rho}\|^2 - 2\|Q\lambda^*_{Q,\rho}\|^2 + 2\rho \\
&= \|Q\lambda\|^2 - \|Q\lambda^*_{Q,\rho}\|^2 + 2\rho,
\end{aligned}$$

which is the desired second inequality in the claim. Hence, the proof is complete. □

Lemma A.4 (Hölder continuity of d_Q w.r.t. Q (Chen et al., 2024)). *For all $Q, Q' \in \mathbb{R}^{d\times M}$, define $\lambda^* \in \arg\min_{\lambda\in\Delta^M} \|Q\lambda\|^2$, and $\lambda^{*\prime} \in \arg\min_{\lambda\in\Delta^M} \|Q'\lambda\|^2$, and $d_Q = Q\lambda^*$, $d'_Q = Q'\lambda^{*\prime}$, then*

$$\|d_Q - d_{Q'}\|^2 \leq 4\max\left\{\sup_{\lambda\in\Delta^M} \|Q\lambda\|, \sup_{\lambda\in\Delta^M} \|Q'\lambda\|\right\} \cdot \sup_{\lambda\in\Delta^M} \|(Q - Q')\lambda\|. \tag{22}$$

Proof. We can first rewrite $\|d_Q - d_{Q'}\|^2 = \|Q\lambda^* - Q'\lambda^{*\prime}\|^2$ as

$$\begin{aligned}
\|Q\lambda^* - Q'\lambda^{*\prime}\|^2 =& \|Q\lambda^*\|^2 + \|Q'\lambda^{*\prime}\|^2 - 2\langle Q\lambda^*, Q'\lambda^{*\prime}\rangle \\
=& \|Q\lambda^*\|^2 - \|Q'\lambda^{*\prime}\|^2 + 2\langle Q'\lambda^{*\prime}, Q'\lambda^{*\prime} - Q\lambda^*\rangle \\
=& \|Q\lambda^*\|^2 - \|Q'\lambda^{*\prime}\|^2 + \underbrace{2\langle Q'\lambda^{*\prime}, Q'\lambda^{*\prime} - Q'\lambda^*\rangle}_{\leq 0} + 2\langle Q'\lambda^{*\prime}, Q'\lambda^* - Q\lambda^*\rangle
\end{aligned}$$

where $\langle Q'\lambda^{*\prime}, Q'\lambda^{*\prime} - Q'\lambda^*\rangle \leq 0$ by (18) in Lemma A.3. Then it can be further bounded by

$$\begin{aligned}
\|Q\lambda^* - Q'\lambda^{*\prime}\|^2 &\overset{(a)}{\leq} \min_{\lambda\in\Delta^M} \|Q\lambda\|^2 - \min_{\lambda\in\Delta^M} \|Q'\lambda\|^2 + 2\|Q'\lambda^{*\prime}\|\|(Q'-Q)\lambda^*\| \\
&= -\max_{\lambda\in\Delta^M} -\|Q\lambda\|^2 + \max_{\lambda\in\Delta^M} -\|Q'\lambda\|^2 + 2\|Q'\lambda^{*\prime}\|\|(Q'-Q)\lambda^*\| \\
&\overset{(b)}{\leq} \max_{\lambda\in\Delta^M} \big(\|Q\lambda\|^2 - \|Q'\lambda\|^2\big) + 2\|Q'\lambda^{*\prime}\|\|(Q'-Q)\lambda^*\| \\
&\overset{(c)}{\leq} \max_{\lambda\in\Delta^M} \|(Q-Q')\lambda\|\big(\|Q\lambda\| + \|Q'\lambda\|\big) + 2\|Q'\lambda^{*\prime}\|\|(Q'-Q)\lambda^*\| \\
&\leq 4\max\Big\{\sup_{\lambda\in\Delta^M}\|Q\lambda\|, \sup_{\lambda\in\Delta^M}\|Q'\lambda\|\Big\}\cdot \sup_{\lambda\in\Delta^M}\|(Q-Q')\lambda\|
\end{aligned}$$

where (a) follows from Cauchy-Schwarz inequality; (b) follows from subadditivity of maximum operator; (c) follows from triangle inequality. The proof is complete. □

A.6 Proof on the convergence rate of Algorithm 1 with random ordering

The following theorem studies the convergence rate of Algorithm 1 with random ordering.

Theorem A.5. *Set* $\alpha = \min\left\{\sqrt{\frac{24\Delta}{KLT\sum_{k=1}^K \sigma_k^2}}, \frac{1}{\sqrt{2}KL}, \frac{1}{AL^2K^2T^{1/3}}\right\}$, *with* random *yields:*

$$\frac{1}{T}\sum_{t=0}^{T-1}\mathbb{E}\|\nabla\mathcal{L}(\boldsymbol{w}_t)\|_2^2 \leq \sqrt{\frac{24L\Delta}{KT}\sum_{k=1}^K\sigma_k^2} + \frac{48L\Delta B^2}{\frac{T}{K}\sum_{k=1}^K\sigma_k^2},$$

To prove theorem A.5, we first need the following lemma:

Lemma A.6. *Suppose that Assumption 3.4 holds. Then for iterates* $\boldsymbol{w}_t$ *generated by Algorithm 1 with stepsize* $\alpha \leq \frac{1}{Ln}$, *we have*

$$\mathcal{L}(\boldsymbol{w}_{t+1}) \leq \mathcal{L}(\boldsymbol{w}_t) - \frac{\alpha K}{2}\|\nabla\mathcal{L}(\boldsymbol{w}_t)\|^2 + \frac{\alpha L_2^2}{K}V_i + \frac{\alpha^2 L}{2}\sum_{k=1}^K\sigma_k^2, \tag{23}$$

where we define $V_t = \sum_{k=1}^K\left\|\boldsymbol{w}_t - \boldsymbol{w}_t^{(k)}\right\|_\infty^2$

Proof. Recall that $\boldsymbol{w}_{t+1} = \boldsymbol{w}_t - \alpha g_t$, where $g_t = \sum_{i=0}^{n-1}\nabla f_{\pi_i}(\boldsymbol{w}_t^i)$. Using L-smoothness of f, we get

$$\begin{aligned}
\mathbb{E}\mathcal{L}(\boldsymbol{w}_{t+1}) \leq& \mathbb{E}\mathcal{L}(\boldsymbol{w}_t) - \alpha K\mathbb{E}\left\langle\nabla\mathcal{L}(\boldsymbol{w}_k), \frac{1}{K}\sum_{k=1}^K\nabla\ell(\boldsymbol{w}_k^{(t)};\xi_{\sigma_k(t)})\right\rangle + \frac{\alpha^2K^2L}{2}\mathbb{E}\left\|\frac{1}{n}\sum_{t=1}^n\nabla\ell(\boldsymbol{w}_k^{(t)};\xi_{\sigma_k(t)})\right\|^2 \\
=& \mathbb{E}\mathcal{L}(\boldsymbol{w}_k) - \frac{\alpha K}{2}\|\nabla\mathcal{L}(\boldsymbol{w}_k)\|^2 - \frac{\alpha n}{2}\left\|\frac{1}{K}\sum_{k=1}^K\nabla\mathcal{L}_k(\boldsymbol{w}_k^{(t)})\right\|^2 \\
&+ \frac{\alpha K}{2}\left\|\nabla\mathcal{L}(\boldsymbol{w}_k) - \frac{1}{K}\sum_{k=1}^K\nabla\mathcal{L}_k(\boldsymbol{w}_k^{(t)})\right\|^2 + \frac{\alpha^2n^2L}{2}\mathbb{E}\left\|\frac{1}{K}\sum_{k=1}^K\nabla\ell(\boldsymbol{w}_k^{(t)};\xi_{\sigma_k(t)})\right\|^2 \\
\leq& \mathbb{E}\mathcal{L}(\boldsymbol{w}_k) - \frac{\alpha K}{2}\|\nabla\mathcal{L}(\boldsymbol{w}_k)\|^2 + \frac{\alpha n}{2}\left\|\nabla\mathcal{L}(\boldsymbol{w}_k) - \frac{1}{K}\sum_{k=1}^K\nabla\mathcal{L}_k(\boldsymbol{w}_k^{(t)})\right\|^2 + \frac{\alpha^2L}{2}\sum_{k=1}^K\sigma_k^2.
\end{aligned}$$

Then we note that:

$$\begin{aligned}\left\|\nabla\mathcal{L}(\boldsymbol{w}_t)-\frac{1}{K}\sum_{k=1}^{K}\nabla\mathcal{L}_k(\boldsymbol{w}_t^{(k)})\right\|^2 =&\left\|\frac{1}{K}\sum_{k=1}^{K}\nabla\mathcal{L}_k(\boldsymbol{w}_t)-\frac{1}{K}\sum_{k=1}^{K}\nabla\mathcal{L}_k(\boldsymbol{w}_t^{(k)})\right\|^2\\ \leq&\frac{1}{K}\sum_{k=1}^{K}\left\|\nabla\mathcal{L}_k(\boldsymbol{w}_t)-\nabla\mathcal{L}_k(\boldsymbol{w}_t^{(k)})\right\|^2\\ \leq&\frac{1}{K}\sum_{k=1}^{K}L_2^2\left\|\boldsymbol{w}_t-\boldsymbol{w}_t^{(k)}\right\|_\infty^2\\ \leq&\frac{L_2^2}{K}V_i,\end{aligned}$$

which complete our proof. □

Lemma A.7. *Suppose that Assumption 3.4 holds and that Algorithm 1 is used with a stepsize $\alpha \leq \frac{1}{2LK}$. Then*

$$\mathbb{E}[V_t] \leq \alpha^2K^3\|\nabla f(\boldsymbol{w}_t)\|^2+\alpha^2K^2\varsigma^2, \tag{24}$$

where V_t is defined as $V_t=\sum_{k=1}^{K}\|\boldsymbol{w}_t-\boldsymbol{w}_t^{(k)}\|_\infty^2$.

Proof. Let us fix any $k\in[1,K-1]$ and find an upper bound for $\mathbb{E}_t\|\boldsymbol{w}_t^k-\boldsymbol{w}_t\|^2$. First, note that

$$\boldsymbol{w}_t^k=\boldsymbol{w}_t-\alpha\sum_{i=0}^{k-1}\nabla\ell(\boldsymbol{w}_t^i,\xi_t^i).$$

Therefore, by Young's inequality, Jensen's inequality and gradient Lipschitzness

$$\begin{aligned}\mathbb{E}_t\|\boldsymbol{w}_t^k-\boldsymbol{w}_t\|^2 &= \alpha^2\mathbb{E}_t\left\|\sum_{i=0}^{k-1}\nabla\ell(\boldsymbol{w}_t^i,\xi_t^i)\right\|^2\\ &\leq 2\alpha^2\mathbb{E}_t\left\|\sum_{i=0}^{k-1}\left(\nabla\ell(\boldsymbol{w}_t^i,\xi_t^i)-\nabla\ell(\boldsymbol{w}_t,\xi_t^i)\right)\right\|^2+2\alpha^2\mathbb{E}_t\left\|\sum_{i=0}^{k-1}\nabla\ell(\boldsymbol{w}_t,\xi_t^i)\right\|^2\\ &\leq 2\alpha^2k\sum_{i=0}^{k-1}\mathbb{E}_t\|\nabla\ell(\boldsymbol{w}_t^i,\xi_t^i)-\nabla\ell(\boldsymbol{w}_t,\xi_t^i)\|^2+2\alpha^2\mathbb{E}_t\left\|\sum_{i=0}^{k-1}\nabla\ell(\boldsymbol{w}_t,\xi_t^i)\right\|^2\\ &\leq 2\alpha^2L^2k\sum_{i=0}^{k-1}\mathbb{E}_t\|\boldsymbol{w}_t^i-\boldsymbol{w}_t\|^2+2\alpha^2\mathbb{E}_t\left\|\sum_{i=0}^{k-1}\nabla\ell(\boldsymbol{w}_t,\xi_t^i)\right\|^2.\end{aligned}$$

Let us bound the second term. For any i we have $\mathbb{E}_t[\nabla\ell(\boldsymbol{w}_t,\xi_t^i)]=\nabla\mathcal{L}(\boldsymbol{w}_t)$, so using (with vectors $\nabla f_{\pi_0}(x_t),\nabla f_{\pi_1}(x_t),\ldots,\nabla f_{\pi_{k-1}}(x_t)$) we obtain

$$\begin{aligned}\mathbb{E}_t\left\|\sum_{i=0}^{k-1}\nabla\ell(\boldsymbol{w}_t,\xi_t^i)\right\|^2 &= k^2\|\nabla\mathcal{L}(\boldsymbol{w}_t)\|^2+k^2\mathbb{E}_t\left\|\frac{1}{k}\sum_{i=0}^{k-1}(\nabla\ell(\boldsymbol{w}_t,\xi_t^i)-\nabla\mathcal{L}(\boldsymbol{w}_t))\right\|^2\\ &\leq k^2\|\nabla\mathcal{L}(\boldsymbol{w}_t)\|^2+\frac{k(K-k)}{K-1}(\varsigma+\max_k\sigma_k)^2.\end{aligned}$$

Combining the produced bounds yields

$$\begin{aligned}\mathbb{E}_t\|\boldsymbol{w}_t^k-\boldsymbol{w}_t\|^2 &\leq 2\alpha^2L^2k\sum_{i=0}^{k-1}\mathbb{E}_t\|\boldsymbol{w}_t^i-\boldsymbol{w}_t\|^2+2\alpha^2k^2\|\nabla f(x_t)\|^2+2\alpha^2\frac{k(K-k)}{K-1}(\varsigma+\max_k\sigma_k)^2\\ &\leq 2\alpha^2L^2k\mathbb{E}[V_t]+2\alpha^2k^2\|\nabla f(x_t)\|^2+2\alpha^2\frac{k(K-k)}{K-1}(\varsigma+\max_k\sigma_k)^2,\end{aligned}$$

whence

$$\mathbb{E}[V_t] = \sum_{k=0}^{K-1} \mathbb{E}_t\|\boldsymbol{w}_t^k - \boldsymbol{w}_t\|^2$$
$$\leq \alpha^2 L^2 K(K-1)\mathbb{E}[V_t] + \frac{1}{3}\alpha^2(K-1)K(2K-1)\|\nabla f(x_t)\|^2 + \frac{1}{3}\alpha^2 K(K+1)(\varsigma + \max_k \sigma_k)^2.$$

Since $\mathbb{E}[V_t]$ appears in both sides of the equation, we rearrange and use that $\alpha \leq \frac{1}{2LK}$ by assumption, which leads to

$$\begin{aligned}\mathbb{E}[V_t] &\leq \frac{4}{3}(1-\alpha^2L^2n(n-1))\mathbb{E}[V_t] \\ &\leq \frac{4}{9}\alpha^2(n-1)n(2n-1)\|\nabla\mathcal{L}(\boldsymbol{w}_t)\|^2 + \frac{4}{9}\alpha^2 n(n+1)\sigma_t^2 \\ &\leq \alpha^2 n^3\|\nabla\mathcal{L}(\boldsymbol{w}_t)\|^2 + \alpha^2 n^2(\varsigma + \max_k \sigma_k)^2.\end{aligned}$$

□

Now we are ready to prove theorem A.5:

Proof. Taking expectation in Lemma A.6 and then using A.7, we have that for any $t \in \{0, 1, \ldots, T-1\}$,

$$\begin{aligned}\mathbb{E}_t[\mathcal{L}(\boldsymbol{w}_{t+1})] &\overset{(23)}{\leq} \mathcal{L}(\boldsymbol{w}_t) - \frac{\alpha K}{2}\|\nabla\mathcal{L}(\boldsymbol{w}_t)\|^2 + \alpha L^2\mathbb{E}_t[V_t] + \frac{\alpha^2 L}{2}\sum_{k=1}^K \sigma_k^2 \\ &\overset{(24)}{\leq} \mathcal{L}(\boldsymbol{w}_t) - \frac{\alpha K}{2}\|\nabla\mathcal{L}(\boldsymbol{w}_t)\|^2 + \alpha L^2(\alpha^2K^3\|\nabla\mathcal{L}(\boldsymbol{w}_t)\|^2 + \alpha^2K^2(\varsigma + \max_k \sigma_k)^2) + \frac{\alpha^2 L}{2}\sum_{k=1}^K \sigma_k^2 \\ &= \mathcal{L}(\boldsymbol{w}_t) - \frac{\alpha K}{2}(1-\alpha^2L^2K^2)\|\nabla\mathcal{L}(\boldsymbol{w}_t)\|^2 + \alpha^3L^2K^2(\varsigma + \max_k \sigma_k)^2 + \frac{\alpha^2 L}{2}\sum_{k=1}^K \sigma_k^2.\end{aligned}$$

Let $\delta_t = \mathcal{L}(\boldsymbol{w}_t) - \mathcal{L}^*$. Adding $-\mathcal{L}^*$ to both sides will give us:

$$\begin{aligned}\mathbb{E}_t[\delta_{t+1}] &\leq \delta_t - \frac{\alpha K}{2}(1-\alpha^2L^2K^2)\|\nabla\mathcal{L}(\boldsymbol{w}_t)\|^2 + \alpha^3L^2K^2(\varsigma + \max_k \sigma_k)^2 + \frac{\alpha^2 L}{2}\sum_{k=1}^K \sigma_k^2 \\ &\leq (1+\alpha^3AL^2K^2)\delta_t - \frac{\alpha K}{2}(1-\alpha^2L^2K^2)\|\nabla\mathcal{L}(\boldsymbol{w}_t)\|^2 + \alpha^3L^2K^2(\varsigma + \max_k \sigma_k)^2 + \frac{\alpha^2 L}{2}\sum_{k=1}^K \sigma_k^2.\end{aligned}$$

Taking unconditional expectations in the last inequality and using that by assumption on α we have $1 - \alpha^2L^2K^2 \geq \frac{1}{2}$, we get the estimate

$$\mathbb{E}[\delta_{t+1}] \leq (1+\alpha^3AL^2K^2)\mathbb{E}(\delta_t) - \frac{\alpha K}{4}\mathbb{E}[\|\nabla\mathcal{L}(\boldsymbol{w}_t)\|^2] + \alpha^3L^2K^2(\varsigma + \max_k \sigma_k)^2 + \frac{\alpha^2 L}{2}\sum_{k=1}^K \sigma_k^2. \tag{25}$$

Then we have:

$$\min_{t=0,\ldots,T-1} \mathbb{E}[\|\nabla\mathcal{L}(\boldsymbol{w}_t)\|^2] \leq \frac{4(1+\alpha^3AL^2K^2)^T}{\alpha KT}(\mathcal{L}(\boldsymbol{w}_0) - \mathcal{L}^*) + 2\alpha^2L^2K(\varsigma + \max_k \sigma_k)^2 + \frac{\alpha L}{2}\sum_{k=1}^K \sigma_k^2.$$

Using that $1 + x \leq \exp(x)$ and that the stepsize α satisfies $\alpha \leq (AL^2K^2T)^{-1/3}$, we have

$$(1+\alpha^3AL^2K^2)^T \leq \exp(\alpha^3AL^2K^2T) \leq \exp(1) \leq 3.$$

Using this in the previous bound, we finally obtain

$$\min_{t=0,\ldots,T-1} \mathbb{E}[\|\nabla\mathcal{L}(\boldsymbol{w}_t)\|^2] \leq \frac{12(\mathcal{L}(\boldsymbol{w}_0) - \mathcal{L}^*)}{\alpha KT} + 2\alpha^2L^2K(\varsigma + \max_k \sigma_k)^2 + \frac{\alpha L}{2}\sum_{k=1}^K \sigma_k^2.$$

□

B Details on Experimental Setup

All experiments are conducted on a server with an Intel Xeon Gold 6342 CPU and an NVIDIA RTX A6000 GPU. We use the PyTorch version 1.10.1 with CUDA version 11.7. For experiments on the NYUv2 data set, we train a Multi-Task Attention Network (MTAN) (Liu et al., 2019) following previous works on multi-task learning (Yu et al., 2020; Navon et al., 2022). We also follow the training procedure from (Liu et al., 2019; Yu et al., 2020; Navon et al., 2022). Each method is trained for 200 epochs with the Adam optimizer (Kingma & Ba, 2015). We set the learning rate $\alpha = 1 \times 10^{-4}$ at the beginning of training, and reduce it to 5×10^{-5} after 100 epochs. The batch size is set to 2 for all methods.

For experiments on QM9 data set, we use the MPNN model proposed in (Gilmer et al., 2017). Each method is trained for 300 epochs with the Adam optimizer (Kingma & Ba, 2015) and we set the learning rate $\alpha = 1 \times 10^{-4}$ throughout the whole training process. The batch size is set to 120 for all methods.

C Comparison of Different Sample Ordering Approaches

To better demonstrate the differences between the three approaches in Figure 1, here we introduce the detailed procedures for the other two approaches. Algorithm 3 describes the procedure for the approach in Figure 1(b) (which orders the training samples for each objective separately). The key difference is that we solve the online vector balancing problem for each objective separately, which introduces separate $\boldsymbol{s}_m$ and $\boldsymbol{v}_{m,t}$'s compared to the unified $\boldsymbol{s}$ and $\boldsymbol{v}_t$ in JoGBa (Algorithm 1).

Algorithm 3 Multi-objective optimization with separate data ordering on each objective (Figure 1(b)).

Input: number of epochs T, initialized order π_1, initialized weight $\boldsymbol{w}_0$, stale mean $\boldsymbol{v}_{m,0} = \boldsymbol{0}$ for all objective $m = 1, \dots, M$, step size α.
for $t = 0, \dots, T-1$ **do**
  for $m = 1, \dots, M$ **do**
    Initialize left index $l_m \leftarrow 1$, right index $r_m \leftarrow K$
  end for
  Initialize running average $\boldsymbol{s}_m \leftarrow \boldsymbol{0}$ for each objective $m = 1, \dots, M$, stale mean $\boldsymbol{v}_{m,t+1} \leftarrow \boldsymbol{0}$.
  for $k = 1, \dots, K$ **do**
    Sample data $\xi_{\pi_t^1(k)}, \dots, \xi_{\pi_t^M(k)}$ from data set $\mathcal{D}$
    for $m = 1, \dots, M$ **do**
      Compute gradient $\nabla \ell_m(\boldsymbol{w}_t^{(k)}; \xi_{\pi_t^m(k)})$ and centered gradient $\boldsymbol{g}_{m,k,t} \leftarrow \nabla \ell_m(\boldsymbol{w}_t^{(k)}; \xi_{\pi_t^m(k)}) - \boldsymbol{v}_{m,t}$
      Compute sign for the current gradient: $\epsilon_{m,k,t} \leftarrow \texttt{Balancing}(\boldsymbol{s}_m, \boldsymbol{g}_{m,k,t})$
      if $\epsilon_{m,k,t} = +1$ **then**
        Update $\boldsymbol{s}_m$ and left index l_m: $\boldsymbol{s}_m \leftarrow \boldsymbol{s}_m + \boldsymbol{g}_{m,k,t}$; $\pi_{t+1}^m(l_m) \leftarrow \pi_t^m(k)$; $l_m \leftarrow l_m + 1$.
      else
        Update $\boldsymbol{s}_m$ and right index r_m: $\boldsymbol{s}_m \leftarrow \boldsymbol{s}_m - \boldsymbol{g}_{m,k,t}$; $\pi_{t+1}^m(r_m) \leftarrow \pi_t^m(k)$; $r_m \leftarrow r_m - 1$.
      end if
      Update stale mean $\boldsymbol{v}_{m,t+1} \leftarrow \boldsymbol{v}_{m,t+1} + \frac{1}{K} \nabla \ell_m(\boldsymbol{w}_t^{(k)}; \xi_{\pi_t^m(k)})$
    end for
    Compute weights λ from multi-task learning algorithms $\lambda = \text{MTL}(\{\nabla \ell_m(\boldsymbol{w}_t^{(k)}; \xi_{\pi_t^m(k)})\}_{m=1}^M)$
    Optimizer Step: $\boldsymbol{w}_t^{(k+1)} \leftarrow \boldsymbol{w}_t^{(k)} - \alpha \sum_{m=1}^M \lambda_m \nabla \ell_m(\boldsymbol{w}_t^{(k)}; \xi_{\pi_t^m(k)})$
  end for
  $\boldsymbol{w}_{t+1}^{(1)} \leftarrow \boldsymbol{w}_t^{(K+1)}$.
end for

Algorithm 4 shows the procedure for the approach in Figure 1(a) (which uses a shared sample order for all objectives). In other words, we use the weighted average of all loss gradients as the sample "gradient", and follow existing data ordering methods on the weighted gradient. When the objective weights do not change with different samples, this extension can be regarded as using the weighted objective as the only objective in the existing methods. However, using the same sample order cannot well tackle the possible conflicts between different objectives.

Algorithm 4 Multi-objective optimization with a shared data order (Figure 1(a)).

Input: number of epochs T, initialized order π_1, initialized weight $\boldsymbol{w}_0$, stale mean $\boldsymbol{v}_0 = \mathbf{0}$, step size α.
for $t = 0, \dots, T-1$ **do**
  for $m = 1, \dots, M$ **do**
    Initialize left index $l_m \leftarrow 1$, right index $r_m \leftarrow K$
  end for
  Initialize running average $\boldsymbol{s} \leftarrow \mathbf{0}$, stale mean $\boldsymbol{v}_{t+1} \leftarrow \mathbf{0}$.
  for $k = 1, \dots, K$ **do**
    Sample data $\xi_{\pi_t^1(k)}, \dots, \xi_{\pi_t^M(k)}$ from data set $\mathcal{D}$
    for $m = 1, \dots, M$ **do**
      Compute gradient $\nabla \ell_m(\boldsymbol{w}_t^{(k)}; \xi_{\pi_t^m(k)})$
    end for
    Compute weights λ from multi-task learning algorithms $\lambda = \text{MTL}(\{\nabla \ell_m(\boldsymbol{w}_t^{(k)}; \xi_{\pi_t^m(k)})\}_{m=1}^M)$
    Compute centered aggreagated gradient $\boldsymbol{g}_{k,t} \leftarrow \sum_{m=1}^M \lambda_m \nabla \ell_m(\boldsymbol{w}_t^{(k)}; \xi_{\pi_t^m(k)}) - \boldsymbol{v}_t$
    Compute sign for the current aggregated gradient: $\epsilon_{k,t} \leftarrow \texttt{Balancing}(\boldsymbol{s}, \boldsymbol{g}_{k,t})$
    for $m = 1, \dots, M$ **do**
      if $\epsilon_{k,t} = +1$ **then**
        Update $\boldsymbol{s}$ and left index l_m: $\boldsymbol{s} \leftarrow \boldsymbol{s} + \boldsymbol{g}_{k,t}$; $\pi_{t+1}^m(l_m) \leftarrow \pi_t^m(k)$; $l_m \leftarrow l_m + 1$.
      else
        Update $\boldsymbol{s}$ and right index r_m: $\boldsymbol{s} \leftarrow \boldsymbol{s} - \boldsymbol{g}_{k,t}$; $\pi_{t+1}^m(r_m) \leftarrow \pi_t^m(k)$; $r_m \leftarrow r_m - 1$.
      end if
    end for
    Update stale mean $\boldsymbol{v}_{t+1} \leftarrow \boldsymbol{v}_{t+1} + \frac{1}{K} \sum_{m=1}^M \lambda_m \nabla \ell_m(\boldsymbol{w}_t^{(k)}; \xi_{\pi_t^m(k)})$
    Optimizer Step: $\boldsymbol{w}_t^{(k+1)} \leftarrow \boldsymbol{w}_t^{(k)} - \alpha \sum_{m=1}^M \lambda_m \nabla \ell_m(\boldsymbol{w}_t^{(k)}; \xi_{\pi_t^m(k)})$
  end for
  $\boldsymbol{w}_{t+1}^{(1)} \leftarrow \boldsymbol{w}_t^{(K+1)}$.
end for

D PLOTS OF GRADIENT NORMS

Figure 5 shows the log-log plot of $\min_{\lambda \in \Delta^M} \|\nabla \mathcal{L}(\boldsymbol{w}_T^{(1)})\lambda\|^2$ with respect to the number of epochs T for different dynamic weighting methods on NYUv2 data set. Recall that Theorem 3.6 demonstrate that the convergence rate is $\mathcal{O}(T^{-1/2})$ for random data ordering, and Theorem 3.9 demonstrate that the convergence rate $\mathcal{O}(T^{-2/3})$ for our method JoGBa. That should correspond to two lines with slope $-\frac{1}{2}$ and $-\frac{2}{3}$ respectively on the log-log plot, as we have also plot these two lines in the figures for better reference. We can see that empirical results on both random ordering and our method JoGBa matches our theoretical results well, which also demonstrate that JoGBa achieves faster convergence compared to the random ordering baseline.

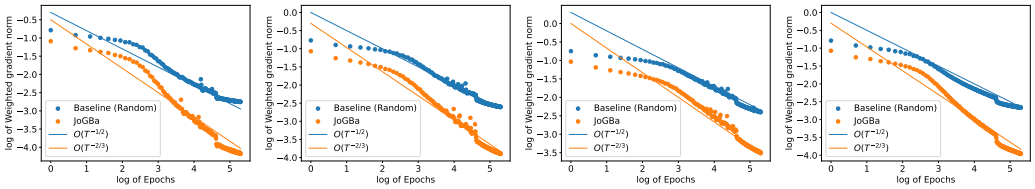

(a) MGDA. (b) CAGrad. (c) PCGrad. (d) Nash-MTL.

Figure 5: Log of weighted gradient norm $\min_{\lambda \in \Delta^M} \|\nabla \mathcal{L}(\boldsymbol{w}_t^{(1)})\lambda\|^2$ for NYUv2 data with different data ordering methods.